L-type prostaglandin D synthase regulates the trafficking of the PGD$_2$ DP1 receptor by interacting with the GTPase Rab4

Chantal Binda[‡§1], Samuel Génier[‡§2], Jade Degrandmaison[‡§1], Samuel Picard[‡§¶3], Louis Fréchette[‡§1], Steve Jean[∥], Eric Marsault[§¶], and Jean-Luc Parent[‡§4]

From the ‡Département de Médecine, §Institut de Pharmacologie de Sherbrooke, ∥Département d'Anatomie et de Biologie Cellulaire, and ¶Département de Pharmacologie-Physiologie, Faculté de Médecine et des Sciences de la Santé, Université de Sherbrooke, Sherbrooke, Québec J1H 5N4, Canada

Edited by Henrik G. Dohlman

Accumulating evidence indicates that G protein–coupled receptors (GPCRs) interact with Rab GTPases during their intracellular trafficking. How GPCRs recruit and activate the Rabs is unclear. Here, we report that depletion of endogenous L-type prostaglandin D synthase (L-PGDS) in HeLa cells inhibited recycling of the prostaglandin D$_2$ (PGD$_2$) DP1 receptor (DP1) to the cell surface after agonist-induced internalization and that L-PGDS overexpression had the opposite effect. Depletion of endogenous Rab4 prevented L-PGDS–mediated recycling of DP1, and L-PGDS depletion inhibited Rab4-dependent recycling of DP1, indicating that both proteins are mutually involved in this pathway. DP1 stimulation promoted its interaction through its intracellular C terminus with Rab4, which was increased by L-PGDS. Confocal microscopy revealed that DP1 activation induces L-PGDS/Rab4 co-localization. L-PGDS/Rab4 and DP1/Rab4 co-immunoprecipitation levels were increased by DP1 agonist treatment. Pulldown assays with purified GST-L-PGDS and His$_6$-Rab4 indicated that both proteins interact directly. L-PGDS interacted preferentially with the inactive, GDP-locked Rab4S22N variant rather than with WT Rab4 or with constitutively active Rab4Q67L proteins. Overexpression and depletion experiments disclosed that L-PGDS partakes in Rab4 activation following DP1 stimulation. Experiments with deletion mutants and synthetic peptides revealed that amino acids 85–92 in L-PGDS are involved in its interaction with Rab4 and in its effect on DP1 recycling. Of note, GTPγS loading and time-resolved FRET assays with purified proteins suggested that L-PGDS enhances GDP-GTP exchange on Rab4. Our results reveal how L-PGDS, which produces the agonist for DP1, regulates DP1 recycling by participating in Rab4 recruitment and activation.

Prostaglandin D$_2$ (PGD$_2$)[5] is a lipid mediator involved in numerous physiological processes, such as bronchoconstriction, vasodilatation (1), sleep (2), and pain (3). It is also implicated in inflammatory responses, such as asthma (4) and atherosclerosis (5). PGD$_2$ exhibits anti-inflammatory properties as well (6–8) and can promote bone formation (9, 10). PGD$_2$ is formed from arachidonic acid through the action of cyclooxygenases (COXs). COXs convert arachidonic acid released from membranes to PGH$_2$, which is metabolized by two types of PGD$_2$ synthase (PGDS). The hematopoietic PGDS (H-PGDS) is GSH-dependent (11) and is mainly expressed in mast cells (12), megakaryocytes (13), and T-helper 2 lymphocytes (14). On the other hand, the lipocalin-type PGDS (L-PGDS) is GSH-independent and is expressed abundantly in the central nervous system (15, 16), the heart (17), the retina (18), and the genital organs (19). L-PGDS is also the only enzyme among the members of the lipocalin gene family and binds small lipophilic substances like retinoic acid (20), bilirubin (21), and gangliosides (22).

PGD$_2$ activates two different G protein–coupled receptors (GPCRs), the D prostanoid receptor (DP1) and CRTH2 (chemoattractant receptor-homologous molecule expressed on Th2 cells, also known as DP2). DP1 is a member of the family of prostanoid receptors (23). On the other hand, CRTH2 is a member of the chemoattractant receptor family, sharing higher sequence homology with the fMLP and C5a receptors than with the prostanoid receptor family (24). GPCRs, which are among the most abundant membrane proteins, respond to a host of stimuli, including light, hormones, lipids, neurotransmitters, and odorants, to induce various physiological responses (25). They share a common molecular topology constituting of a hydrophobic core of seven transmembrane α-helices, three intracellular loops, three extracellular loops, an extracellular N

[5] The abbreviations used are: PGD$_2$, prostaglandin D$_2$; COX, cyclooxygenase; PGDS, prostaglandin D synthase; H- and L-PGDS, hematopoietic and lipocalin-type PGDS, respectively; GPCR, G protein–coupled receptor; DsiRNA, Dicer-substrate siRNA; HATU, hexafluorophosphate azabenzotriazole tetramethyl uronium; DIPEA, N,N-diisopropylethylamine; TIPS, triisopropylsilane; EDT, 1,2-ethanedithiol; GAP, GTPase-activating protein; GEF, guanine nucleotide exchange factor; β$_2$AR, β$_2$-adrenergic receptor; GST, GSH-S-transferase; ICL, intracellular loop; GTPγS, guanosine 5′-3-O-(thio)triphosphate; TR, time-resolved; DMEM, Dulbecco's modified Eagle's medium; TBS, Tris-buffered saline; Fmoc, N-(9-fluorenyl)methoxycarbonyl; HA, hemagglutinin; GAPDH, glyceraldehyde-3-phosphate dehydrogenase.

ASBMB

J. Biol. Chem. (2019) 294(45) 16865–16883 **16865**

terminus, and an intracellular C terminus. GPCRs are generally delivered to the plasma membrane in a ligand-responsive and signaling-competent form. Following agonist stimulation, the majority of GPCRs internalize into endosomes from which they can undergo recycling to the cell surface or lysosomal degradation (26–30).

We and others have shown that GPCRs interact with small Rab GTPases (Rabs) to control their trafficking (26, 31–37). However, the interacting partners involved in the assembly of GPCR-Rab complexes and in the activation of Rabs that are important for the correct routing of a given GPCR remain poorly characterized. With over 60 known members, Rabs form the largest branch of the Ras-related small GTPase family (38–41). Rabs have been identified as key regulators of numerous cellular processes that determine, for example, cell shape, motility, differentiation, and growth. They are also involved at almost every level of vesicle-mediated transport (42, 43). Depending on their cellular function, each Rab has a distinct subcellular localization, enabling the efficient transport of cargo proteins between compartments (42, 44). To accomplish their roles, Rabs alternate between a GDP-bound inactive and a GTP-bound active form (45, 46). When Rabs are activated, they can anchor to a specific membrane or vesicle, where they regulate its trafficking (47, 48). GTPase-activating proteins (GAPs) are needed to counteract the slow intrinsic GTPase activity of Rabs and to allow rapid cycling to their inactive states by favoring GTP hydrolysis (48, 49). In their inactive forms, Rabs are tightly bound to GDP, and the dissociation of the nucleotide is a slow process. Guanine nucleotide exchange factors (GEFs) accelerate the conversion of Rab GTPases from the inactive to the active form (50). Because there is a higher cytosolic concentration of GTP than GDP, GTP binds quickly after the GDP is dislodged, which in turn displaces the GEF to yield the active GTP-bound form (50, 51). Other mechanisms of Rab GTPase activation have been reported, such as phosphorylation and ubiquitinition (26, 52).

We have shown previously that DP1 is recycled back to the plasma membrane following internalization via Rab4-positive recycling endosomes (53). Rab4 plays a pivotal role in the rapid recycling of numerous key cargo proteins back to the cell surface, such as integrins, receptors, ubiquitin ligases, proteases, and channels (41). Accumulating evidence indicates that Rab4 is required for cancer cell invasion (51, 54–58) by regulating the recycling of furin (59), $\beta 3$ integrin, and MT1-MMP, leading to invadosome formation, degradation, and remodeling of the extracellular matrix (60). Given its biological importance, it is surprising that the mechanisms of Rab4 activation are still largely unknown.

Our prior work showed that L-PGDS interacts with DP1 and directs the anterograde transport of the receptor by acting as a co-factor of the Hsp90 molecular chaperone (61). The purpose of the present study was to investigate the possible role of L-PGDS in Rab4-dependent recycling of DP1. Our intriguing findings indicate that L-PGDS, an enzyme that synthesizes PGD_2, regulates the recycling of the DP1 receptor for PGD_2 by recruiting and activating Rab4.

Results

L-PGDS regulates the recycling of DP1

We previously reported that L-PGDS interacts directly with DP1 and is involved in the anterograde trafficking of the receptor (61). As such, we were interested in determining whether it also takes part in other aspects of DP1 trafficking. Two cell types were used throughout our experiments: 1) HeLa cells because they endogenously express DP1, L-PGDS, and Rab4 and produce PGD_2 (61) and 2) human embryonic kidney 293 (HEK293) cells for studies that involved L-PGDS overexpression because they express low levels of endogenous L-PGDS protein. We assessed the involvement of L-PGDS in agonist-induced internalization of DP1. HeLa cells stably expressing FLAG-tagged DP1 and transfected with control or L-PGDS–specific siRNAs (61) were used to perform cell-surface ELISAs (26, 61–64). Time-course analyses showed that the depletion of L-PGDS significantly increases the agonist-induced internalization of DP1 by roughly 50% (Fig. 1*A*). These results were confirmed with the use of a second L-PGDS siRNA (Fig. 1*B*). Cell-surface detection assays of DP1 were also conducted using HEK293 cells. Time-course analyses showed that the overexpression of L-PGDS results in a ~30% decrease in DP1 agonist-induced internalization after 120 min of stimulation (Fig. 1*C*). Parallel experiments were conducted to verify whether L-PGDS acts in a similar fashion with respect to the β_2-adrenergic receptor (β_2AR), the prototypical GPCR. Overexpression of L-PGDS had no effect on the agonist-induced internalization of FLAG-tagged β_2AR in HEK293 cells (Fig. 1*D*).

Given that an increase in receptor recycling can decrease the detected percentage of receptor internalization, recycling time-course experiments were conducted to determine whether L-PGDS regulates DP1 recycling. Cells were stimulated with 1 μM PGD_2 for 30 min to promote receptor internalization and were then incubated in agonist-free culture medium for various times to allow receptor recycling. L-PGDS increased DP1 recycling 2-fold after 15 min of agonist removal (Fig. 1*E*). We previously showed that L-PGDS is involved in the assembly of an Hsp90–L-PGDS–DP1 complex that is required for receptor export to the cell surface (61). We thus tested the L-PGDS W43A/G47A mutant, defective in binding to Hsp90 (61), to determine whether the involvement of L-PGDS in DP1 recycling is due to its Hsp90 co-factor activity. The L-PGDS W43A/G47A mutant promoted DP1 recycling (Fig. 1*E*) and reduced agonist-induced internalization of DP1 (Fig. 1*F*) similarly to WT L-PGDS, suggesting that L-PGDS plays a role in the recycling of DP1 that is independent of its association with Hsp90.

L-PGDS and Rab4 play mutually dependent roles in regulating DP1 recycling

GPCRs are internalized by vesicles at the plasma membrane, which deliver them to early endosomes. The receptors are then either targeted to degradation pathways or are recycled back to the cell membrane for further activation via Rab4-positive endosomes or Rab11-positive endosomes (64–68). Our previous work showed that DP1 is recycled via Rab4-positive endosomes but not by the Rab11-dependent recycling pathway (53). We thus investigated the role of L-PGDS in the Rab4-dependent
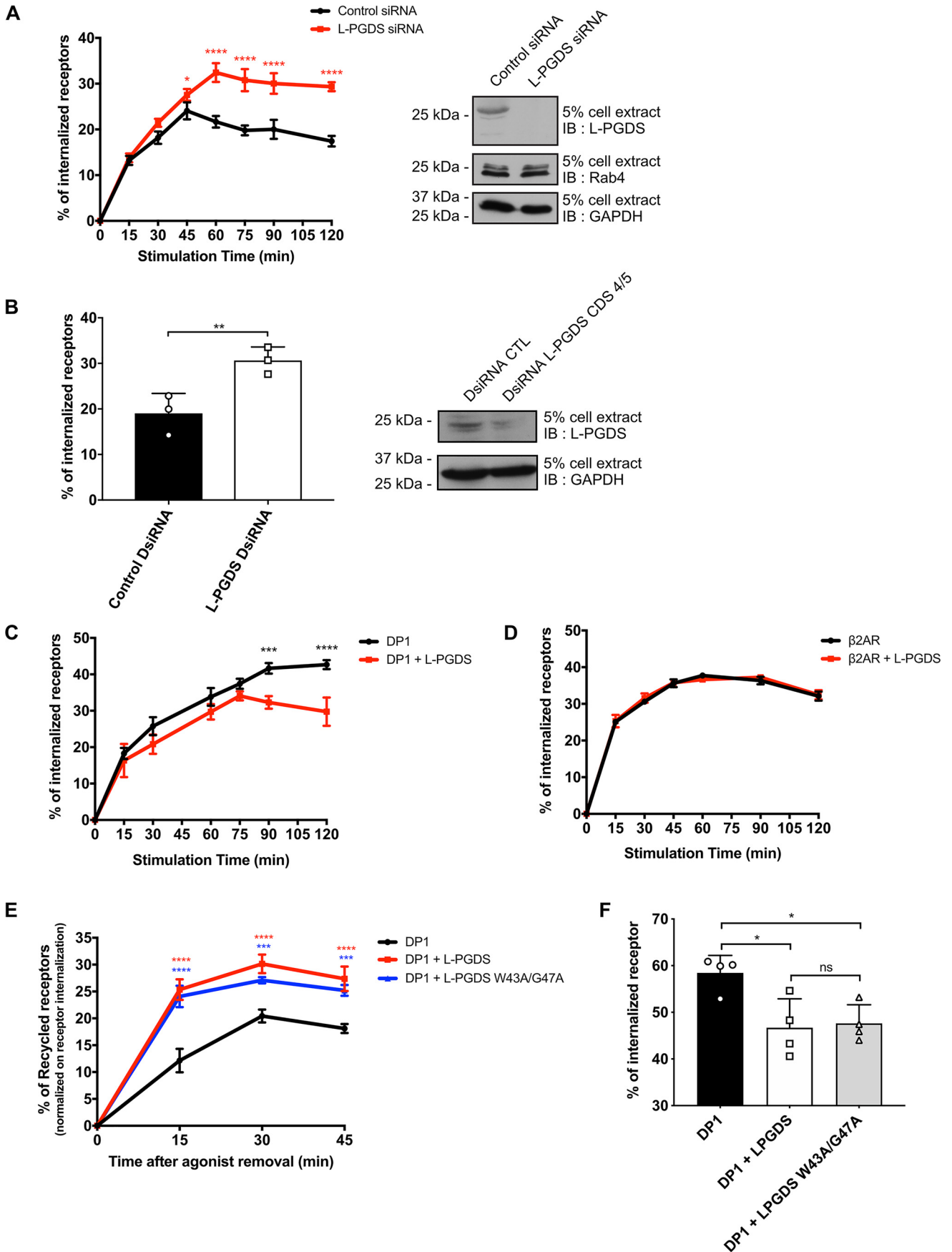
recycling of DP1. First, we performed a cell-surface expression assay using HEK293 cells that had been stimulated with PGD_2 for 2 h and calculated the percentage of internalized receptors when L-PGDS and Rab4 were co-expressed alone or together (Fig. 2A). The overexpression of L-PGDS decreased the agonist-induced internalization of DP1 by ~30% compared with the internalization of DP1 alone (Fig. 2A, *column 2 versus column 1*), similar to what was observed in Fig. 1. The expression of Rab4 decreased DP1 internalization by 27% (Fig. 2A, *column 3 versus column 1*). Interestingly, the co-expression of L-PGDS and Rab4 resulted in a 52% decrease in DP1 internalization (Fig. 2A, *column 4 versus column 1*).

To determine whether the involvement of L-PGDS in DP1 recycling is Rab4-dependent, we transfected HEK293 cells with control or Rab4-specific DsiRNAs. The cells were stimulated with PGD_2 for 2 h prior to cell-surface expression assays. Knockdown of Rab4 expression reduces DP1 recycling, leading to the detection of increased agonist-induced internalization of the receptor. As can be seen in Fig. 2B (*column 3 versus column 1*), Rab4 depletion increased DP1 agonist-induced internalization by 26% compared with the control. Furthermore, the ability of L-PGDS to decrease DP1 internalization by 31% (Fig. 2B, *column 2 versus column 1*) in the presence of the control DsiRNA was abrogated by Rab4 depletion (Fig. 2B, *column 4 versus column 3*). Similar data were obtained with a second Rab4 DsiRNAs (Fig. 2C). These results suggest that Rab4 is required for L-PGDS to play its role in DP1 recycling.

We then verified whether the effect of Rab4 on DP1 recycling depended on L-PGDS. Using an L-PGDS–specific siRNA, we assessed the functional involvement of endogenous L-PGDS in the internalization of DP1 in HeLa cells stably expressing the FLAG-tagged receptor that had been transfected with Rab4. Depletion of L-PGDS increased the percentage of internalized receptors by 26% compared with the control siRNA (Fig. 2D, *column 3 versus column 1*), confirming the results shown in Fig. 1A. The promotion of DP1 recycling by the co-expression of Rab4 reduced agonist-induced receptor internalization by 21% in the presence of a control siRNA (Fig. 2D, *column 2 versus column 1*), which was abrogated by the depletion of L-PGDS (Fig. 2D, *column 4 versus column 3*). Finally, it can be seen in Fig. 2E that Rab4 depletion reduces DP1 recycling after agonist-induced internalization, confirming the data we obtained before (53). Taken together, these results indicate that L-PGDS and Rab4 play mutually dependent roles in the regulation of DP1 recycling.

Rab4 co-localizes with L-PGDS upon DP1 stimulation

Our previous confocal microscopy studies showed that DP1 and L-PGDS are present in vesicular structures in the cytoplasm and mainly co-localize in the perinuclear region (61) and that DP1 displayed strong co-localization with Rab4 following PGD_2 stimulation of DP1 (53). Confocal microscopy performed in HeLa cells revealed that L-PGDS and Rab4 weakly co-localize in basal conditions as depicted in the *top panels* of Fig. 3. L-PGDS is mainly localized in vesicular structures "surrounding" the Rab4-positive compartments, reflected by the fluorogram showing clear distinction between the *red* and *green pixels*. Stimulation of DP1 with PGD_2 induced a redistribution of L-PGDS and enhanced noticeably its co-localization with Rab4 (Fig. 3, *bottom panels*) as shown by the increase in co-localizing *yellow pixels* in the *insets*.

## L-PGDS promotes the interaction between Rab4 and DP1

We and others have shown that trafficking of GPCRs can be mediated by their interactions with Rabs (31–33, 35–37, 64–67). To investigate the interaction between DP1, L-PGDS, and Rab4 in a cellular context, we performed immunoprecipitation assays on lysates of HEK293 cells expressing FLAG-DP1, L-PGDS-MYC, or HA-Rab4 with a FLAG-specific mAb (Fig. 4A). The co-immunoprecipitation of Rab4 with DP1 was detected in both the absence and presence of L-PGDS co-expression and was promoted by PGD_2 stimulation over time. Of note, the co-expression of L-PGDS increased the DP1-Rab4 interaction by 75 and 65% after 60 and 120 min of stimulation, respectively (Fig. 4A, *top panel* and *densitometry graph*). As we reported previously (61), the DP1–L-PGDS interaction was not modulated by agonist stimulation (Fig. 4A, *second panel* from *top*).

We then determined whether the DP1-Rab4 interaction could be direct. We performed *in vitro* binding assays using purified DP1 intracellular domains fused to GSH-*S*-transferase (GST) and purified Rab4 fused to a hexahistidine tag (His$_6$-Rab4). As indicated by the results presented in Fig. 4B, Rab4 mainly interacts directly with the C terminus of DP1 and, more weakly, with the first intracellular loop (ICL1), but not with ICL2 or ICL3. We then investigated the possibility that L-PGDS modulates this interaction because our previous work revealed that L-PGDS can also interact directly with the DP1 C terminus (61). We used the purified GST-DP1-C terminus construct to conduct *in vitro* binding assays using cell lysates of HEK293

Figure 1. DP1 recycling is increased by L-PGDS. *A* and *B*, HeLa cells stably expressing FLAG-DP1 were transfected with an siRNA targeting L-PGDS (s11446 in *A* and CDS4/5 in *B*) or a negative control siRNA. 72 h post-transfection, cells were stimulated with 1 μM PGD_2 for the indicated times in *A* or for 60 min in *B*. Receptor cell-surface expression was measured by ELISA, and the percentage of receptor internalization was calculated. Cells were harvested as described under "Experimental procedures" to assess protein levels by Western blotting using L-PGDS, Rab4, and GAPDH antibodies. *C*, HEK293 cells were transfected with pcDNA3-FLAG-DP1 alone or in combination with pcDNA3-L-PGDS-HA. 48 h post-transfection, cells were stimulated with 1 μM PGD_2 for the indicated times. Receptor cell-surface expression was measured by ELISA, and the percentage of receptor internalization was calculated. *D*, HEK293 cells were transfected with pcDNA3-FLAG-β_2AR alone or in combination with pcDNA3-L-PGDS-HA. 48 h post-transfection, cells were stimulated with 10 μM isoproterenol for the indicated times. Receptor cell-surface expression was measured by ELISA, and the percentage of receptor internalization was calculated. *E*, HEK293 cells were co-transfected with pcDNA3-FLAG-DP1 and pcDNA3-L-PGDS or pcDNA3-L-PGDS-W43A/G47A, an L-PGDS mutant with reduced binding to Hsp90. Cells were treated with 1 μM PGD_2 for 30 min at 37 °C and then incubated in DMEM for the indicated time periods to prevent further internalization and to allow receptor recycling. Cell-surface expression of the receptor was detected by ELISA, and the percentage of receptor recycling was calculated. *F*, HEK293 cells were transfected with pcDNA3-FLAG-DP1 alone or in combination with pcDNA3-L-PGDS-HA or pcDNA3-L-PGDS-W43A/G47A. 48 h post-transfection, cells were stimulated with 1 μM PGD_2 for 60 min. Receptor cell-surface expression was measured by ELISA, and the percentage of receptor internalization was calculated. Results are means ± S.E. (*error bars*) or means ± S.D. (*error bars*) (for *B* and *F*) of at least three separate experiments. *, $p < 0.05$; **, $p < 0.01$; ***, $p < 0.001$; ****, $p < 0.0001$; *ns*, not significant.

cells expressing HA-Rab4 in the presence or absence of purified His$_6$-L-PGDS. Fig. 4*C* shows that the interaction between Rab4 and the DP1-C terminus is augmented in the presence of L-PGDS. Taken together, these results indicate that the DP1-Rab4 interaction can be direct and is increased by the agonist stimulation of DP1 and by the presence of L-PGDS.
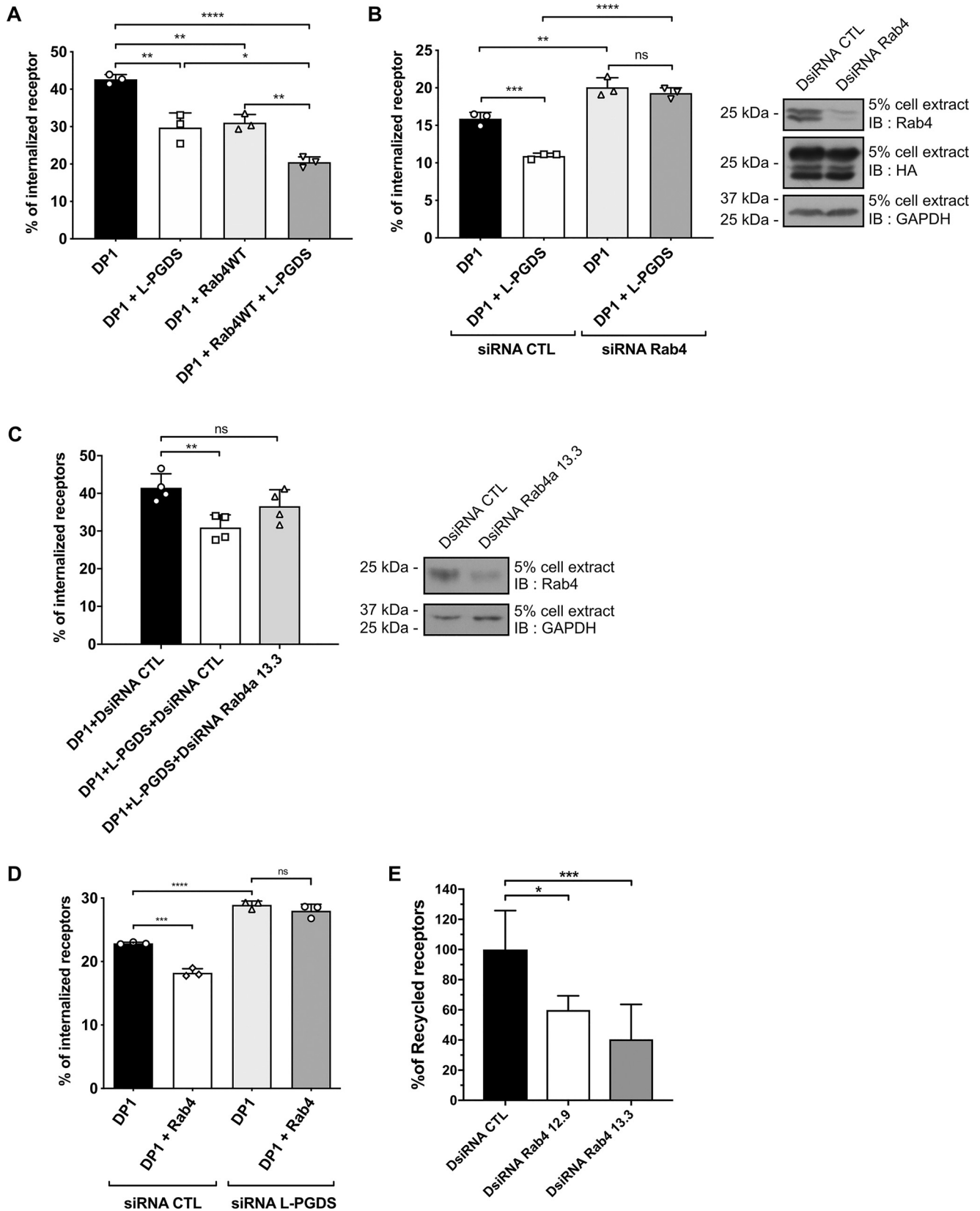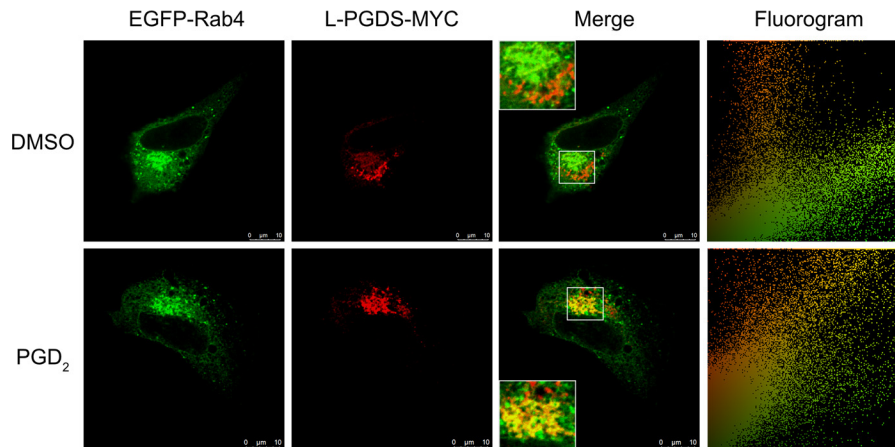
Figure 3. L-PGDS co-localizes intracellularly with Rab4 upon DP1 stimulation. HeLa cells were transiently transfected with pcDNA3-L-PGDS-MYC and pEGFP-C2-Rab4 for 48 h. The cells were then incubated with vehicle (*top*) or with 1 μM PGD$_2$ (*bottom*) for 60 min. The cells were then fixed and prepared for confocal microscopy as indicated under "Experimental procedures." EGFP-Rab4 was visualized using a 488-nm emission laser line and an EGFP detection filter (*green*). L-PGDS was labeled using a MYC-specific polyclonal primary antibody and an Alexa Fluor 633-conjugated anti-rabbit IgG secondary antibody. L-PGDS was visualized using a 633-nm emission laser line and an Alexa Fluor 633 detection filter (*red*). Overlays of the staining patterns of the *green* fluorescent EGFP-Rab4 and the *red*-labeled L-PGDS (*merge*) and the corresponding fluorograms are presented. The areas with a high degree of co-localization appear *yellow*. All laser intensities and acquisition parameters were conserved among the different conditions to allow comparison. The images shown are single confocal slices and are representative of ~200 observed cells over three independent experiments. *Bars*, 10 μM.

L-PGDS interacts directly with Rab4

Given the involvement of L-PGDS in the DP1-Rab4 interaction, we performed immunoprecipitation assays using lysates from HEK293 cells expressing L-PGDS-MYC, HA-Rab4, or FLAG-DP1 and a MYC-specific mAb to determine whether L-PGDS interacts with Rab4. The co-immunoprecipitation of Rab4 was detected by Western blotting using an HA antibody. Interestingly, the interaction between Rab4 and L-PGDS was strongly increased over time when DP1 was stimulated with PGD$_2$ (Fig. 5A), in agreement with the L-PGDS–Rab4 co-localization data from Fig. 3. The L-PGDS–Rab4 interaction was confirmed at native level, where endogenous Rab4 co-immunoprecipitated following the immunoprecipitation of endogenous L-PGDS from HeLa cells (Fig. 5B), which produce PGD$_2$ and express DP1 intrinsically (61). We also performed *in vitro* binding assays using purified L-PGDS fused to GST together with purified His$_6$-Rab4. Fig. 5C reveals that Rab4 bound to GST-L-PGDS but not to GST, showing that L-PGDS can interact directly with Rab4.

Because Rab4 is a GTPase that cycles between inactive GDP-bound and active GTP-bound forms, we were interested in determining whether L-PGDS interacts preferentially with one of the two forms. We performed *in vitro* GST-L-PGDS pulldown assays using lysates of HEK293 cells expressing

HA-Rab4WT, HA-Rab4S22N (GDP-locked, inactive mutant), or HA-Rab4Q67L (GTPase-deficient, constitutively active mutant). The pulldown of Rab4 was detected by Western blotting using an HA antibody (Fig. 5D). Interestingly, L-PGDS displays a strong preference for binding to Rab4S22N over WT Rab4 or Rab4Q67L. Following this result, we questioned whether L-PGDS could interact with GDP-locked mutants of other Rabs. We performed immunoprecipitation assays using a MYC-specific mAb on lysates from HEK293 cells expressing L-PGDS–MYC and various HA-Rabs (Rab4S22N, Rab5S34N, Rab11S25N, Rab1S25N, Rab6T27N, and Rab8T22N). Fig. 5E shows that, among the Rabs that were tested, L-PGDS interacts only with the GDP-locked form of Rab4. These results suggest that the interaction between Rab4 and L-PGDS can be modulated by the agonist stimulation of DP1 and can occur endogenously by a direct protein-protein interaction, preferentially with the GDP-bound form of Rab4.

L-PGDS increases the levels of activated Rab4

We next studied whether DP1 activates Rab4 and if L-PGDS takes part in this mechanism. Rabaptin is an effector of Rab4 that interacts with the GTP-bound form of Rab4, which can be used in pulldown experiments to detect Rab4 activation (68, 69). We performed *in vitro* binding assays using purified GST-

Figure 2. Mutually dependent roles of L-PGDS and Rab4 in regulating DP1 recycling. *A*, HEK293 cells were transfected with pcDNA3-FLAG-DP1, pcDNA3-HA-Rab4, pcDNA3-L-PGDS-MYC, or a combination of constructs as indicated. 48 h post-transfection, cells were stimulated with 1 μM PGD$_2$ for the indicated times. Receptor cell-surface expression was measured by ELISA, and the percentage of receptor internalization was calculated. *B* and *C*, HEK293 cells were transfected with a DsiRNA targeting Rab4 (HSC.RNAI.N004578.12.9 in *B* and HSC.RNAI.N004578.13.3 in *C*) or a DsiRNA negative control. 24 h after DsiRNA transfection, cells were transiently transfected with pcDNA3-FLAG-DP1 and pcDNA3-L-PGDS-HA. 48 h after the second transfection, cells were either stimulated with 1 μM PGD$_2$ for 2 h to measure receptor cell-surface expression by ELISA and calculate the percentage of receptor internalization or harvested as described under "Experimental procedures" to assess protein levels by Western blotting using Rab4, HA, and GAPDH antibodies. *D*, HeLa cells stably expressing FLAG-DP1 were transfected with siRNA s11446 targeting L-PGDS or a siRNA negative control. 24 h after siRNA transfection, cells were transiently transfected with pcDNA3-HA-Rab4WT. 48 h after the second transfection, cells were stimulated with 1 μM PGD$_2$ for 2 h to measure receptor cell-surface expression by ELISA and calculate the percentage of receptor internalization. *E*, HEK293 cells were transfected with a DsiRNA targeting Rab4 or a DsiRNA negative control. 24 h after DsiRNA transfection, cells were transiently transfected with pcDNA3-FLAG-DP1. 48 h after the second transfection, cells were treated with 1 μM PGD$_2$ for 30 min at 37 °C and then incubated in DMEM for the indicated time periods to prevent further internalization and to allow receptor recycling. Cell-surface expression of the receptor was detected by ELISA, and the percentage of receptor recycling was calculated. The mean of the data obtained in the presence of the DsiRNA control was set to 100%. Results are means ± S.D. (*error bars*) of at least three separate experiments. *, $p < 0.05$; **, $p < 0.01$; ***, $p < 0.001$; ****, $p < 0.0001$; *ns*, not significant.
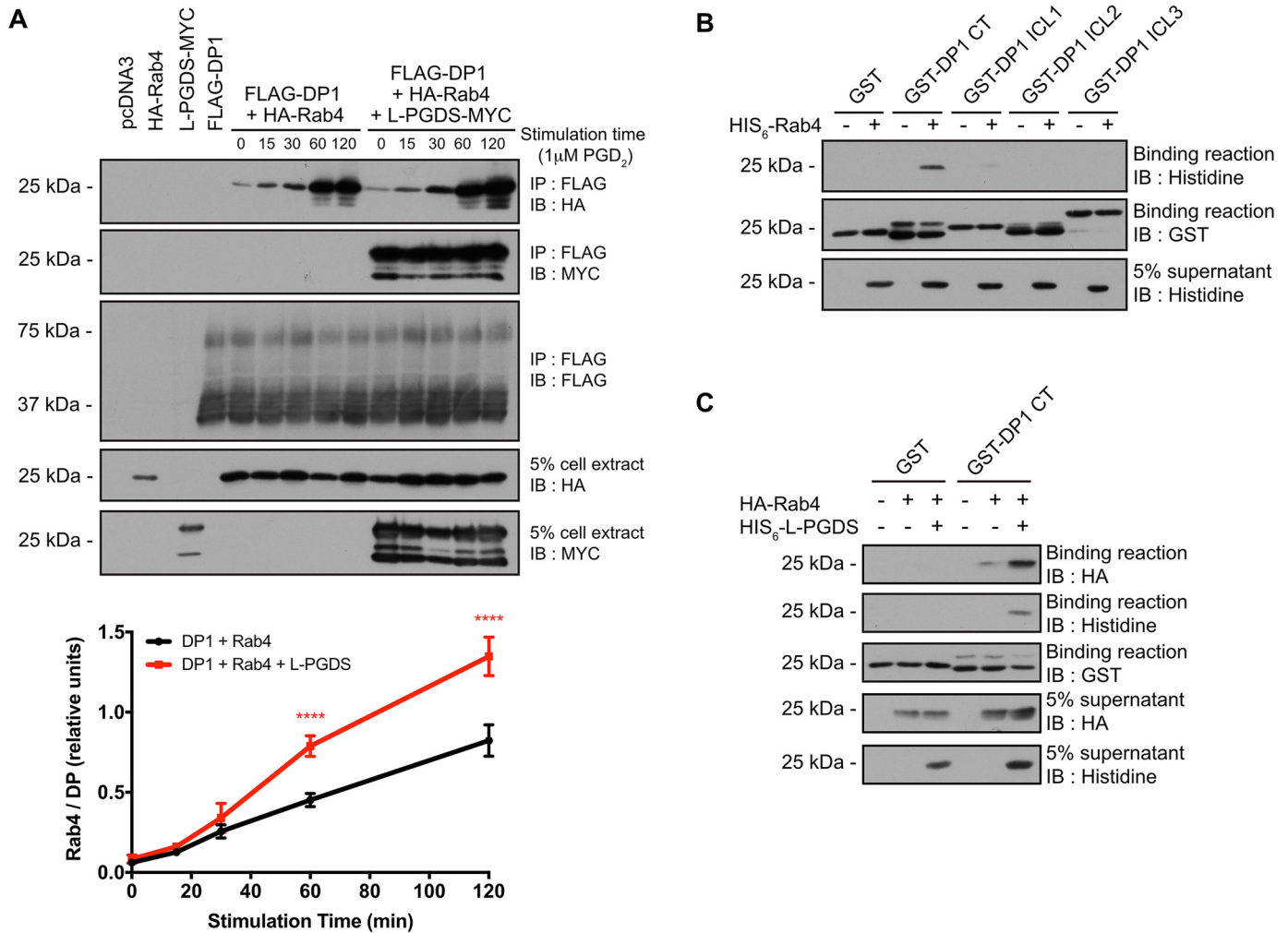
Figure 4. The Rab4-DP1 interaction is promoted by L-PGDS. *A*, HEK293 cells transiently transfected with pcDNA3-FLAG-DP1, pcDNA3-HA-Rab4, pcDNA3-L-PGDS-MYC, or a combination of constructs were stimulated for the indicated times with 1 μM PGD$_2$. Immunoprecipitation (*IP*) of the receptor was performed using a FLAG-specific mAb, and immunoblotting (*IB*) was performed with FLAG-specific polyclonal, peroxidase-conjugated anti-HA or anti-MYC antibodies. The graph shows densitometry analyses performed on four different experiments. Rab4 pixels were normalized on DP1 pixels, and results are presented as the ratio of these values (means ± S.E. (*error bars*)). *B*, binding assays were carried out using purified GSH-Sepharose–bound GST-DP1-CT and intracellular loops (*ICL*) incubated with His$_6$-Rab4. Rab4 binding to the receptor domains was detected by immunoblotting using an anti-His antibody, and the GST fusion proteins present in the binding reaction were detected using an anti-GST antibody. *C*, binding assays were carried out using purified GSH-Sepharose–bound GST-DP1-CT incubated with His$_6$-L-PGDS and a cellular lysate of cells transfected with pcDNA3-HA-Rab4. Rab4 binding to the receptor domains was detected by immunoblotting using an anti-HA antibody, L-PGDS was detected using an anti-His antibody, and the GST fusion proteins were detected using an anti-GST antibody. Blots shown are representative of four independent experiments. ****, $p < 0.0001$.

rabaptin and lysates of HEK293 cells stably expressing DP1 that also expressed HA-Rab4WT alone or in combination with L-PGDS–MYC following a time course of PGD$_2$ stimulation. Fig. 6A shows that Rab4 was weakly activated after 0 and 15 min of DP1 stimulation (*lanes 1* and *2*), followed by a gradual increase in Rab4 activation after 30 min of PGD$_2$ treatment (*lanes 3–5*). A densitometric analysis (Fig. 6A, *bottom panel*) indicated that there is a marked increase in Rab4 activation at the basal level and following stimulation of DP1 with PGD$_2$ when L-PGDS is co-expressed (Fig. 6A, *lanes 6–10*). L-PGDS does not interact with rabaptin (Fig. 6A, *second panel, IB: MYC*). We then verified whether depletion of endogenous L-PGDS reduces Rab4 activation. GST-rabaptin pulldown assays were performed on lysates of HeLa cells stably expressing DP1 that were transfected with the indicated combinations of HA-Rab4WT, control, or L-PGDS–specific siRNAs (Fig. 6B). There was basal activation of Rab4 (Fig. 6B, *lane 1*) that was

strongly increased after 60 and 120 min of DP1 stimulation (*lanes 2* and *3*) when cells were treated with the control siRNA. On the other hand, basal activation of Rab4 was abrogated (Fig. 6B, *lane 4*), and PGD$_2$-induced Rab4 activation was greatly reduced (Fig. 6B, *lanes 5* and *6*) when L-PGDS was depleted. We then carried out *in vitro* GTPγS-loading experiments with purified His$_6$-Rab4 in the absence or presence of purified L-PGDS for times ranging from 0 to 15 min. GTP loading of Rab4 was detected as described above by GST-rabaptin pulldown and Western blotting analyses. Interestingly, L-PGDS increased the GTPγS loading of Rab4 (Fig. 6C), as indicated by enhanced Rab4 binding to rabaptin.

To further study whether L-PGDS can participate in Rab4 activation, we used purified L-PGDS and Rab4 proteins and performed GDP-GTP exchange experiments. The classic assay using Mant-GDP (68, 69) could not be used, as L-PGDS strongly binds Mant-GDP nonspecifically. This could be due to the

L-PGDS interacts with Rab4

Mant moiety, because excess of GDP could not compete with Mant-GDP binding on L-PGDS (data not shown). Therefore, we turned to a Transcreener GDP time-resolved (TR)-FRET assay. The latter bases its principle on the displacement of a GDP HiLyte647 tracer initially bound to a GDP antibody-terbium conjugate by the GDP released by a small GTPase (Fig.

7A). GDP-GTP exchange on the small GTPase leads to the release of GDP in the reaction that displaces the tracer, resulting in a decrease in the TR-FRET signal. Fig. 7B shows that the addition of increasing concentrations of purified L-PGDS to GDP-loaded Rab4 causes a dose-dependent decrease in TR-FRET signals, consistent with the idea that L-PGDS promotes
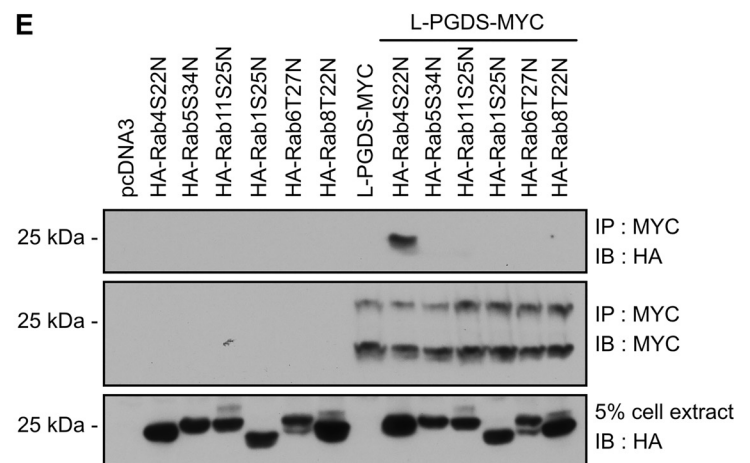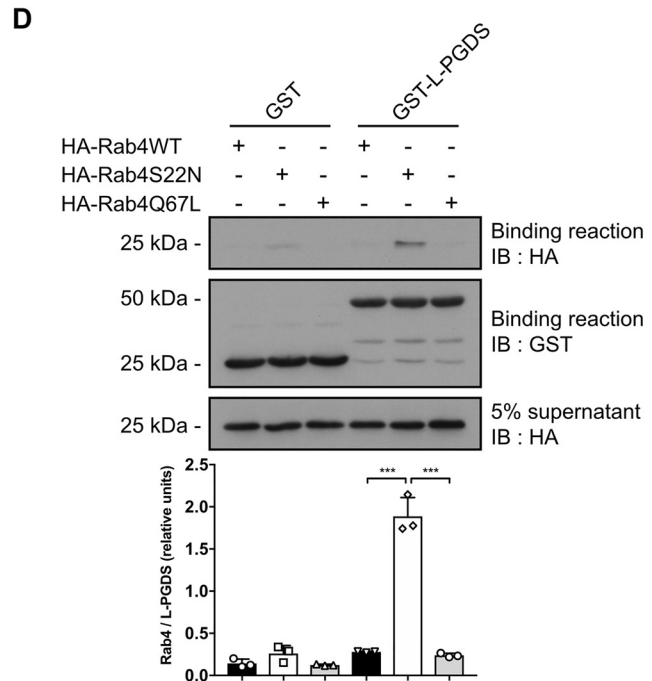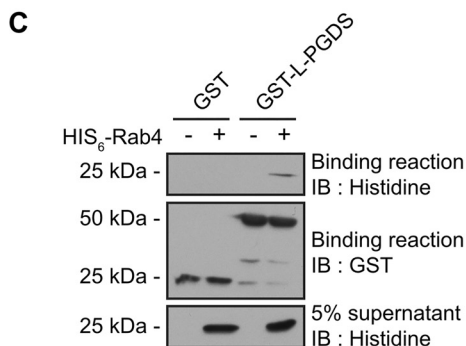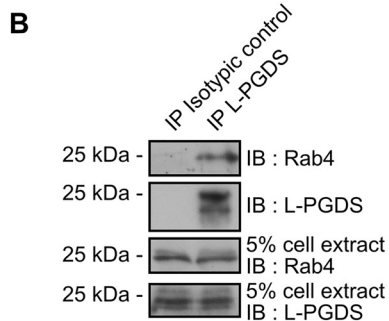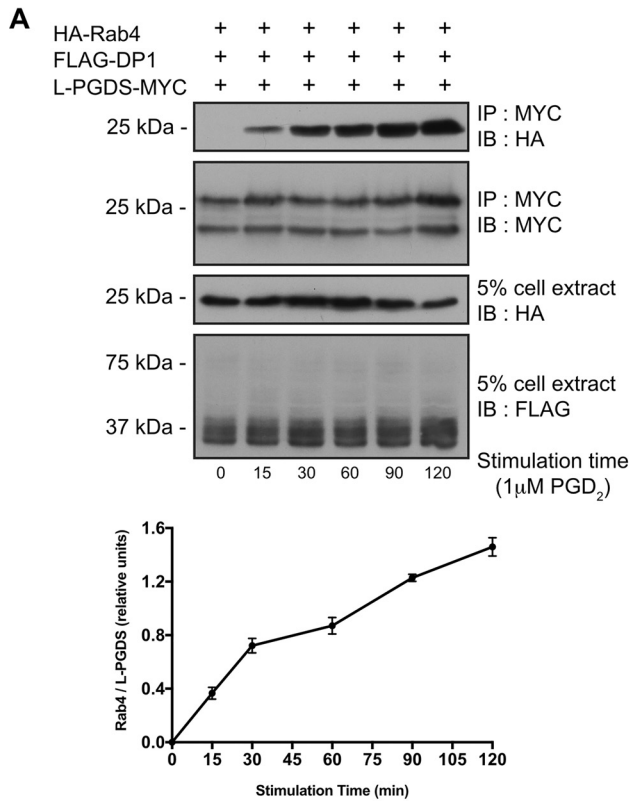
Rab4 activation and GDP release. Time-course assays revealed that the half-time of the GDP-GTP exchange reaction is accelerated in the presence of L-PGDS ($t_{1/2}$ = 42.8 min) compared with Rab4 alone ($t_{1/2}$ = 64.4 min), further suggesting that there is increased Rab4 activation in the presence of L-PGDS (Fig. 7C). Together, these results indicate that L-PGDS can partake in Rab4 activation, but further experiments will be needed to determine the nature of the mechanism involved.

Identification of the Rab4-binding domain on L-PGDS

Our next aim was to identify the L-PGDS domain involved in the interaction with Rab4. To this end, we produced several L-PGDS deletion mutant constructs that were fused to GST (Fig. 8A) and used them in *in vitro* pulldown assays with purified His$_6$-Rab4. The binding reactions were analyzed by immunoblotting using an anti-His mAb to detect the binding of Rab4. As summarized in Fig. 8A, there were no differences among the first five mutants in terms of binding to Rab4 compared with the full-length L-PGDS protein (blots not shown). We then investigated the L-PGDS domain comprising residues 75–98 (Fig. 8B). The L-PGDS structure revealed that the 75–98 and 85–92 amino acid sequences are part of two β strands folded to form an antiparallel β loop protruding from the core of the structure. Because these strands appeared to be accessible for protein interactions, it seemed plausible that they could serve as a Rab4-binding site. Interestingly, our results showed that Rab4 does not interact with the L-PGDS Δ75–98 and Δ85–92 deletion mutants (Fig. 8C).

To further corroborate these results, we produced a construct consisting of amino acids 75–98 of L-PGDS fused with GST. *In vitro* binding assays were carried out using the GST-tagged construct and purified His$_6$-Rab4. As can be seen in Fig. 8D, Rab4 bound to the GST-L-PGDS 75–98 construct but not to GST alone. Moreover, a peptide corresponding to amino acids 78–98 of L-PGDS was synthesized together with its scrambled control peptide. The ^{75}GGK^{77} amino acids were not included in the peptide because of solubility issues. The peptides were preincubated individually with purified His$_6$-Rab4 prior to performing GST-L-PGDS pulldown assays as described above to determine whether they would compete in the L-PGDS–Rab4 interaction. Remarkably, the L-PGDS 78–98 peptide completely abrogated the binding of Rab4 to L-PGDS, whereas the scrambled peptide had no significant effect (Fig. 9A).

Finally, we tested the ability of the Rab4 binding–deficient L-PGDS Δ75–98 and Δ85–92 deletion mutants to promote DP1 recycling. Unlike the WT L-PGDS, the L-PGDS Δ75–98 and Δ85–92 deletion mutants failed to enhance DP1 recycling after agonist-induced internalization in HEK293 cells (Fig. 9B). Altogether, our results indicate that amino acids 78–98 of L-PGDS are involved in Rab4 binding and that the L-PGDS–Rab4 interaction is required for L-PGDS to participate in the recycling of DP1.
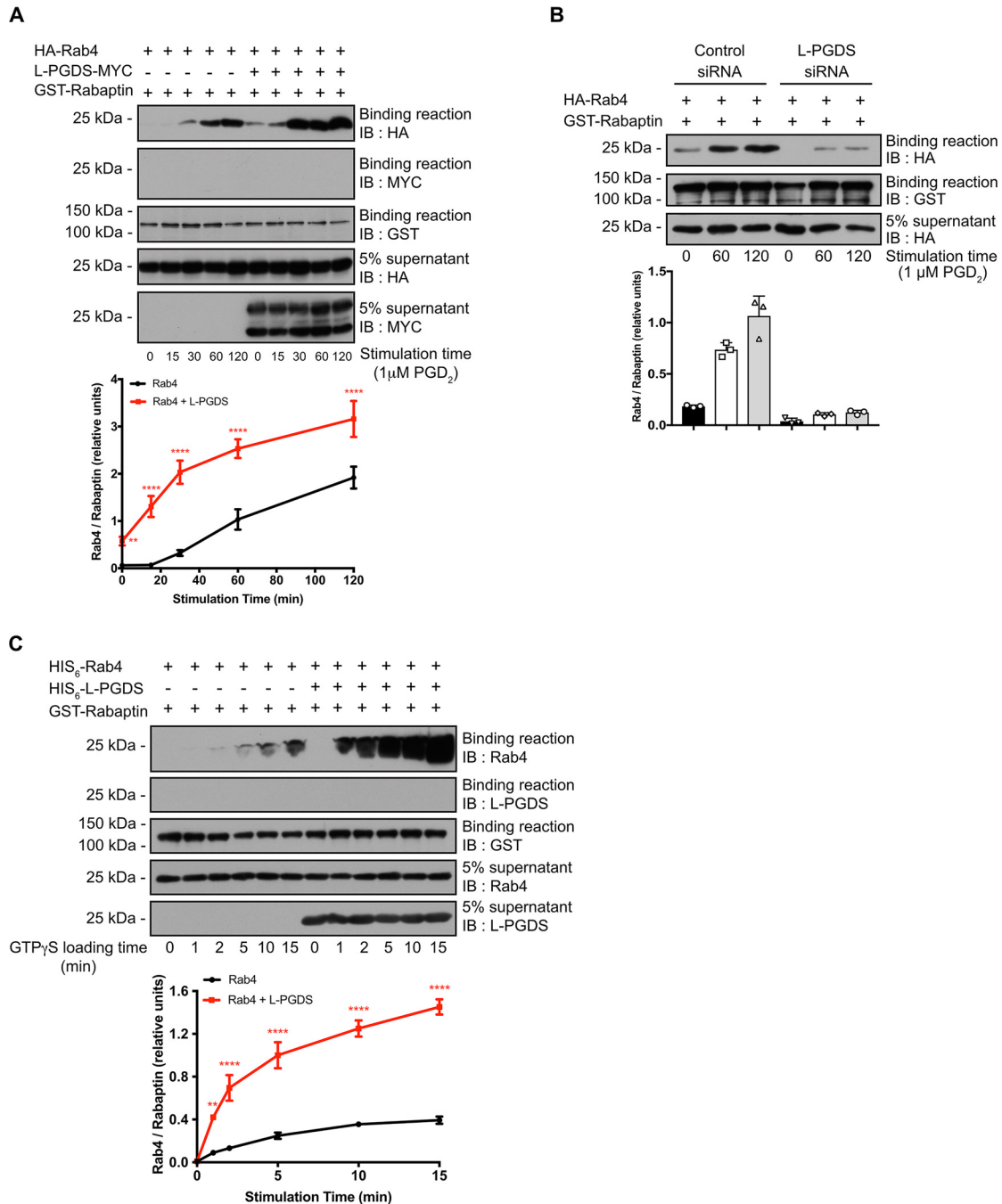
Discussion

To maintain the sensitivity of cells to their environment, it is crucial for receptors to be able to recycle back to the cell surface. We and others have shown that the spatial and temporal vesicular transport of many GPCRs is regulated by direct interactions with various members of the Rab subfamily of small GTPases (32–34, 36, 37, 70–74). The central aspect of Rab GTPase function is their specific localization in distinct subcellular compartments, which makes it possible to precisely control trafficking (75). The mechanisms by which Rabs are recruited to GPCRs in particular membrane compartments are poorly understood.

Like other small GTPases, the spatiotemporal activation and inactivation of Rab GTPases are tightly regulated by GEFs and GAPs (47, 76). Rab4 is a small GTPase that is critical for the recycling of many key cargo proteins. Surprisingly, there is no identified GEF for Rab4, and how it is activated and recruited to cargo proteins is still an open question. In addition to being involved in normal cell physiology, Rab4 may be associated with disease. For example, Rab4 expression is elevated in Alzheimer's disease (77, 78). It has been proposed that Rab4 could be a target for the treatment of systemic lupus erythematosus (79). Accumulating evidence also indicates that Rab4 is involved in tumor growth and metastasis by regulating plasma membrane levels of receptor tyrosine kinases (80), integrins (57), P-glycoprotein in multidrug resistance (81), and proteases (59, 60). It is thus essential to identify Rab4-interacting proteins to better understand the biology of this important small GTPase.

Additional regulatory mechanisms were reported to be involved in the regulation of Rab GTPases activity. For example, Rab4 is regulated by protein kinase A following activation of the β$_2$AR (52). We described previously (26) how a complex between the β$_2$AR and the ubiquitin ligase HACE1 results in Rab11a ubiquitination on Lys-145. This ubiquitination is involved in the activation of Rab11a and in the regulation of β$_2$AR recycling to the plasma membrane (26). Research efforts are also targeted at understanding whether GPCRs interact with other components of the Rab-associated machinery. In this regard, we observed that the interaction between the β$_2$AR and Rab geranylgeranyltransferase modulates the trafficking of

Figure 5. L-PGDS interacts directly with Rab4. *A*, HEK293 cells transiently transfected with pcDNA3-FLAG-DP1, pcDNA3-HA-Rab4, and pcDNA3-L-PGDS-MYC were stimulated for the indicated times with 1 μM PGD$_2$. Immunoprecipitation (*IP*) of L-PGDS was performed using a MYC-specific mAb, and immunoblotting (*IB*) was performed with a peroxidase-conjugated anti-MYC or anti-HA or a FLAG-specific polyclonal antibody. *B*, immunoprecipitation was performed in HeLa cells using L-PGDS–specific monoclonal or rat isotypic control IgG antibodies, and immunoblotting was done using L-PGDS–specific polyclonal or Rab4-specific polyclonal antibodies. *C*, binding assays were carried out using purified GSH-Sepharose– bound GST-L-PGDS incubated with His$_6$-Rab4. The binding of Rab4 to L-PGDS was detected by immunoblotting using an anti-His antibody, and GST-L-PGDS was detected using an anti-GST antibody. *D*, binding assays were carried out using purified GSH-Sepharose-bound GST-L-PGDS incubated with cellular lysates of HEK293 cells transfected with pcDNA3-HA-Rab4WT, pcDNA3-HA-Rab4S22N, or pcDNA3-HA-Rab4Q67L. Rab4 binding to L-PGDS was detected by immunoblotting using an anti-HA antibody. L-PGDS was detected using an anti-GST antibody. *E*, HEK293 cells were transiently transfected with pcDNA3-L-PGDS-MYC and the indicated pcDNA3-HA-Rab constructs. Immunoprecipitation of L-PGDS was performed using a MYC-specific mAb, and immunoblotting was performed with a peroxidase-conjugated anti-MYC or anti-HA. Graphs show densitometry analyses performed on three different experiments. Rab4 pixels were normalized on L-PGDS pixels, and results are presented as -fold of these values (means ± S.D. (*error bars*)). ***, $p < 0.001$.

A

HA-Rab4   + + + + + + + + + +
L-PGDS-MYC   - - - - - + + + + +
GST-Rabaptin + + + + + + + + + +

25 kDa -   Binding reaction IB : HA
25 kDa -   Binding reaction IB : MYC
150 kDa -   Binding reaction IB : GST
100 kDa -
25 kDa -   5% supernatant IB : HA
25 kDa -   5% supernatant IB : MYC

0 15 30 60 120 0 15 30 60 120   Stimulation time (1 μM PGD$_2$)

B

HA-Rab4   + + +   + + +
GST-Rabaptin + + +   + + +

Control siRNA   L-PGDS siRNA

25 kDa -   Binding reaction IB : HA
150 kDa -   Binding reaction IB : GST
100 kDa -
25 kDa -   5% supernatant IB : HA

0 60 120   0 60 120   Stimulation time (1 μM PGD$_2$)

C

HIS$_6$-Rab4   + + + + + + + + + + + +
HIS$_6$-L-PGDS - - - - - - + + + + + +
GST-Rabaptin   + + + + + + + + + + + +

25 kDa -   Binding reaction IB : Rab4
25 kDa -   Binding reaction IB : L-PGDS
150 kDa -   Binding reaction IB : GST
100 kDa -
25 kDa -   5% supernatant IB : Rab4
25 kDa -   5% supernatant IB : L-PGDS

GTPγS loading time (min)   0 1 2 5 10 15   0 1 2 5 10 15

Figure 6. Activation of Rab4 is promoted by L-PGDS. *A*, HEK293 cells stably expressing pcDNA3-FLAG-DP1 were transiently transfected with pcDNA3-HA-Rab4, pcDNA3-L-PGDS-MYC, or a combination of constructs and stimulated for the indicated times with 1 μM PGD$_2$ 48 h post-transfection. Binding assays were carried out using purified GSH-Sepharose–bound GST-rabaptin incubated with these cellular lysates. Rab4 and L-PGDS binding to rabaptin were detected by immunoblotting (*IB*) using a peroxidase-conjugated anti-HA or anti-MYC antibody, respectively. GST-rabaptin was detected using an anti-GST antibody. *B*, HeLa cells stably expressing FLAG-DP1 were transfected with siRNA s11446 targeting L-PGDS or a negative control siRNA. 72 h post-transfection, cells were stimulated with 1 μM PGD$_2$ for the indicated times. Binding assays were carried out using purified GSH-Sepharose–bound GST-rabaptin incubated with these cellular lysates, and binding of active Rab4 was detected by immunoblotting using a peroxidase-conjugated anti-HA antibody. GST-rabaptin was detected using an anti-GST antibody. *C*, GTPγS loading of Rab4 was performed as described under "Experimental procedures" for the indicated periods of time. Binding assays were carried out using purified GSH-Sepharose–bound GST-rabaptin incubated with His$_6$-Rab4, His$_6$-L-PGDS, or a combination of both. The binding of active Rab4 and L-PGDS was detected by immunoblotting using an anti-Rab4 or anti-L-PGDS antibody, and GST-rabaptin was detected using an anti-GST antibody. Graphs show densitometry analyses performed on at least three different experiments. Rab4 pixels were normalized on rabaptin pixels (means ± S.E. (*error bars*) in *A* and *C*, means ± S.D. in *B*). **, $p < 0.01$; ****, $p < 0.0001$.

the receptor and the geranylgeranylation of Rab6a, Rab8a, and Rab11a ([64]).

Our earlier work showed that DP1 recycles to the cell surface through Rab4 after agonist-induced internalization ([53]). In a separate study, we demonstrated that L-PGDS participates in

the anterograde transport of DP1 through an interaction with the receptor and the Hsp90 chaperone. Furthermore, L-PGDS promoted the formation of a DP1-ERK1/2 complex and increased DP1-mediated ERK1/2 signaling. Interestingly, DP1 augmented PGD$_2$ synthesis by L-PGDS, revealing an intracrine
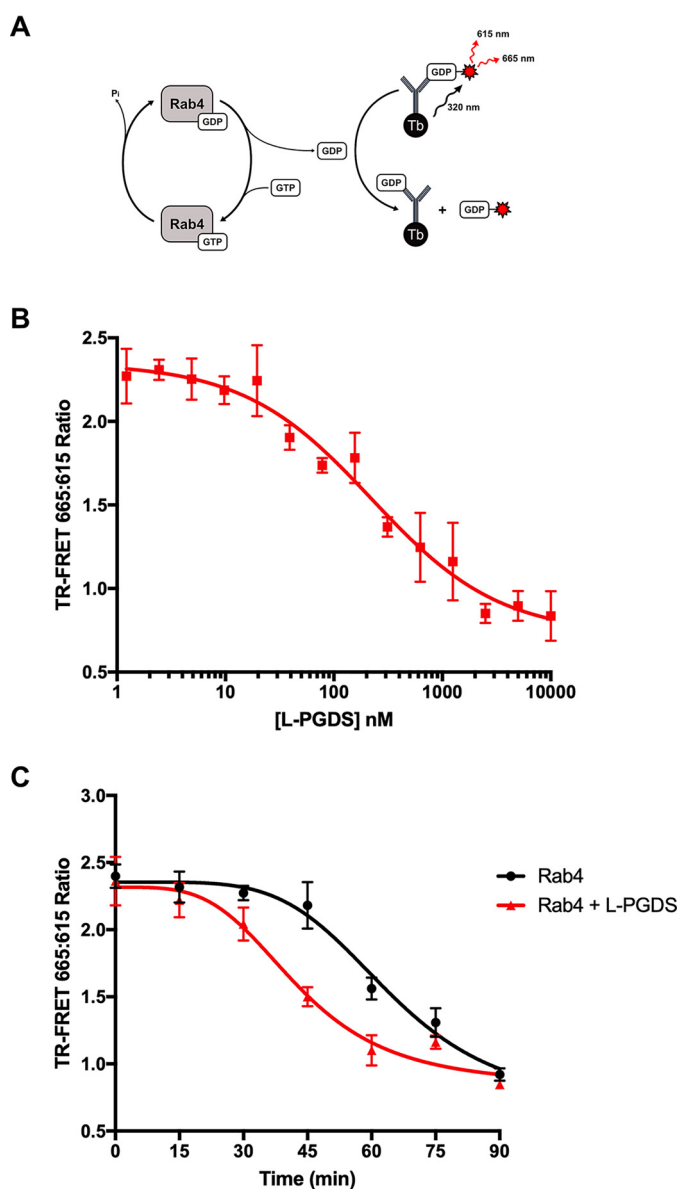
Figure 7. L-PGDS increases nucleotide exchange on Rab4. *A, schematic representation* of the TR-FRET reaction. GDP released by the enzyme reaction displaces a GDP HiLyte647 tracer initially bound to a GDP antibody conjugated to terbium (*Tb*), thus generating a decrease in TR-FRET signal. *B*, titration of L-PGDS ranging from 1 nM to 10 μM was performed in the presence of a fixed Rab4 concentration of 80 nM as described under "Experimental procedures." *C*, time-course assays were carried out for the indicated periods of time. Final concentrations of 80 nM Rab4 and 320 nM L-PGDS were used, and enzyme reactions were performed and stopped, and TR-FRET signal was measured as described under "Experimental Procedures." Graphs are represented as TR-FRET ratios (665/615), and results are means $\pm$ S.E. (*error bars*) of three separate experiments. Data were analyzed with GraphPad Prism using a four-parameter nonlinear regression curve fitting.

signaling loop between DP1 and L-PGDS (61). L-PGDS thus appears as a multifunctional protein capable not only of PGD$_2$ synthesis and transport of lipophilic molecules, but also of regulating protein complex formation involved in DP1 trafficking and signaling. We were thus interested in studying whether L-PGDS is involved in recycling of the DP1 receptor and if this would involve Rab4.

Experiments using overexpression or depletion of endogenous L-PGDS revealed that it regulates DP1 recycling after agonist-induced internalization. Inhibiting endogenous Rab4 expression inhibited the promotion of DP1 recycling by L-PGDS, whereas conversely, knocking down endogenous L-PGDS prevented the Rab4-mediated recycling of DP1. L-PGDS and Rab4 thus appear to work in conjunction with each other in regulating DP1 recycling.

Agonist-induced internalization of DP1 is rather slow compared with other GPCRs. To detect an effect of recycling on receptor internalization after the addition of the agonist, the receptor has to first internalize and then recycle. This may explain why the L-PGDS–mediated recycling effect on DP1 internalization can be observed starting after 30 min of agonist treatment and becomes statistically significant after 90 min of DP1 stimulation. On the other hand, the effect of L-PGDS appears faster in the recycling assays (apparent after 15 min of agonist removal). This may be because in the latter context, the receptor was stimulated for 30 min prior to the recycling measurements, so the system was already "turned on" for 30 min when the recycling measurements began. Furthermore, the agonist is removed in the recycling assays, so the effect of L-PGDS on recycling does not compete with concomitant DP1 internalization, facilitating its detection more rapidly. We cannot totally exclude the possibility that the role of L-PGDS in anterograde transport (61) is involved, at least in part, in regulating replenishment of DP1 to the plasma membrane after agonist-induced internalization. However, the L-PGDS W43A/G47A mutant, defective in the interaction with Hsp90 necessary for L-PGDS to promote anterograde transport (61), had effects similar to those of WT L-PGDS on agonist-induced internalization and recycling of DP1. In contrast, the L-PGDS W43A/G47A mutant had a 70% reduced capacity to promote DP1 anterograde transport compared with WT L-PGDS (61). Altogether, our data support the idea that L-PGDS promotes recycling of DP1 and that its interaction with Hsp90 as well as its role in anterograde trafficking do not play a significant role, if any, in the recycling of DP1.

How Rab GTPases are recruited to particular cargo proteins is poorly characterized. We and others have shown that a number of Rabs interact directly with the C-terminal ends of GPCRs (31–34, 72). The C terminus of DP1 was identified as the interaction site with Rab4, and Rab4 binding was enhanced by agonist stimulation of the receptor and by the presence of L-PGDS. The L-PGDS–Rab4 co-localization and interaction was also promoted by DP1 activation. We confirmed that Rab4 directly binds to L-PGDS using *in vitro* binding assays with purified recombinant proteins. Our data showed that L-PGDS did not bind to the other Rabs tested (Rab1, -5, -8, and -11), suggesting that L-PGDS displays at least a certain degree of specificity toward Rab4. Further experiments will be needed to determine the full extent of the L-PGDS interaction spectrum within the family of Rab GTPases. L-PGDS did not modulate the internalization of the β_2AR, indicating that it does not play a general role in GPCR trafficking.

Like all members of the Ras superfamily, Rab4 cycles between a GDP-bound and a GTP-bound form. Whereas the GDP-bound form is considered inactive, the GTP-bound form binds to effectors, switching on downstream cellular responses (50). Interestingly, our binding assays revealed that L-PGDS prefer-
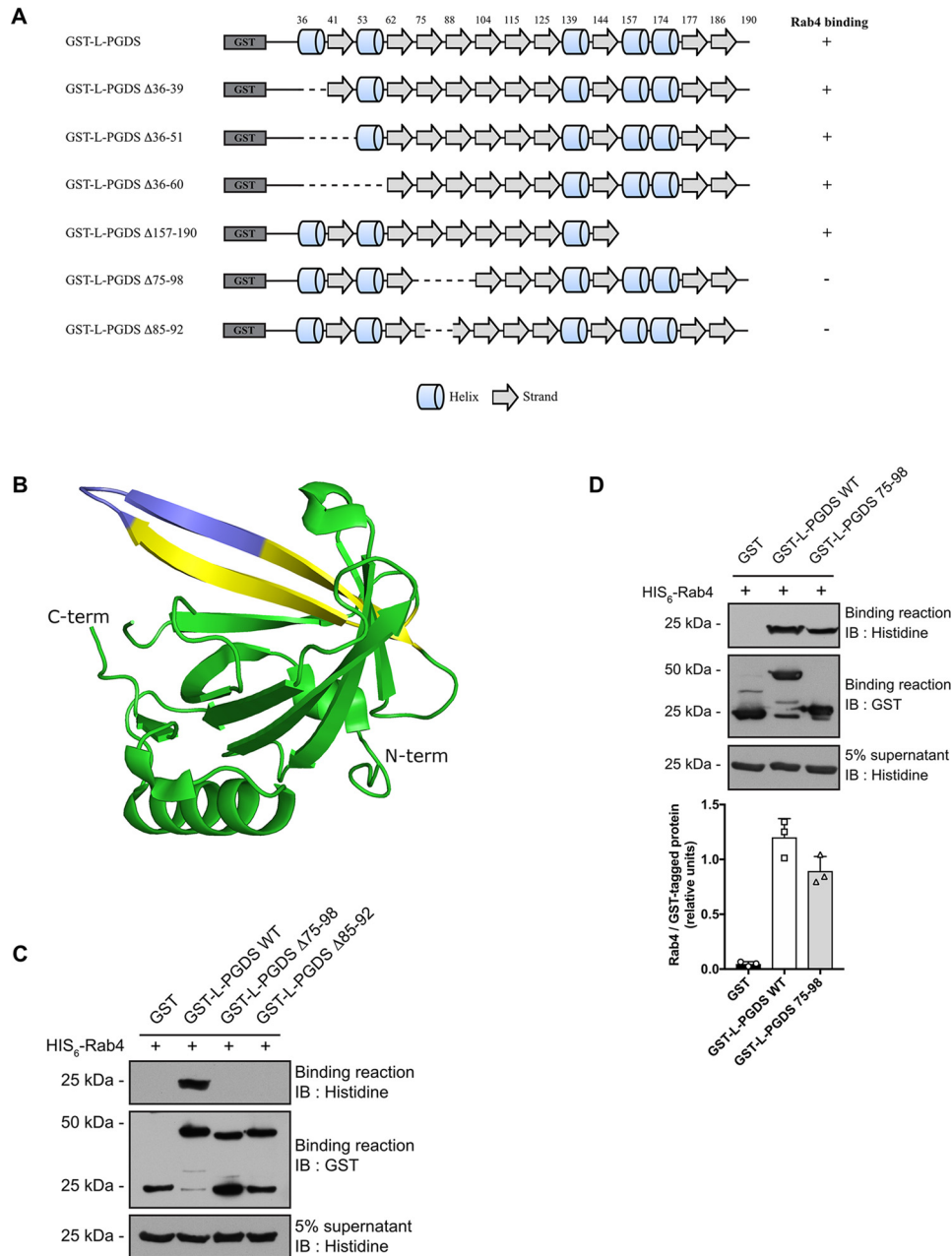
Figure 8. Identification of the L-PGDS region that interacts with Rab4. *A, schematic representation* of the different GST-tagged L-PGDS mutants. The Rab4-binding properties of the L-PGDS constructs are indicated on the *right*. *B,* the illustration of the complete L-PGDS structure (shown in *green*) was prepared with PyMOL (Schrödinger, LLC, New York) using the known crystal structure of L-PGDS (Protein Data Bank entry 2WWP). The two potential Rab4-binding sites are shown in *yellow* (residues 75–98) and *blue* (residues 85–92), respectively. *C,* binding assays were carried out using purified GSH-Sepharose– bound GST-L-PGDS WT or its mutants incubated with His$_6$-Rab4. The binding of Rab4 to L-PGDS was detected by immunoblotting (*IB*) using an anti-His antibody, and GST-L-PGDS was detected using an anti-GST antibody. *D,* binding assays were carried out using purified GSH-Sepharose– bound GST-L-PGDS WT or GST-L-PGDS 75–98 incubated with His$_6$-Rab4. The binding of Rab4 to L-PGDS was detected by immunoblotting using an anti-His antibody, and GST-L-PGDS was detected using an anti-GST antibody. The graph shows densitometry analyses performed on three different experiments. Rab4 pixels were normalized on L-PGDS pixels (means ± S.D. (*error bars*)).

entially interacts with the GDP-bound form of Rab4. Moreover, L-PGDS increased the levels of activated Rab4 in cells following DP1 stimulation, as well as Rab4 GTPγS loading *in vitro* using purified proteins, as reflected by binding to its effector rabaptin. This indicated that L-PGDS may be involved in regulating the activation of Rab4. This was further supported by the stimulation of Rab4 GDP-GTP exchange by L-PGDS *in vitro* using a TR-FRET assay. In a nutshell, we observed that: 1) L-PGDS associates with Rab4 in a time-dependent manner after DP1

stimulation; 2) L-PGDS only binds significantly to the GDP-bound inactive state of Rab4 but is constitutively associated with DP1; 3) L-PGDS favors Rab4 recruitment and activation by DP1; and 4) L-PGDS is not detected in the rabaptin pulldowns. Because the rabaptin pulldowns would only capture active GTP-bound Rab4, this would be consistent with a model in which L-PGDS binds inactive Rab4 and recruits it to the receptor, participates in its activation, and then dissociates. However, additional work will be necessary to characterize the nature of
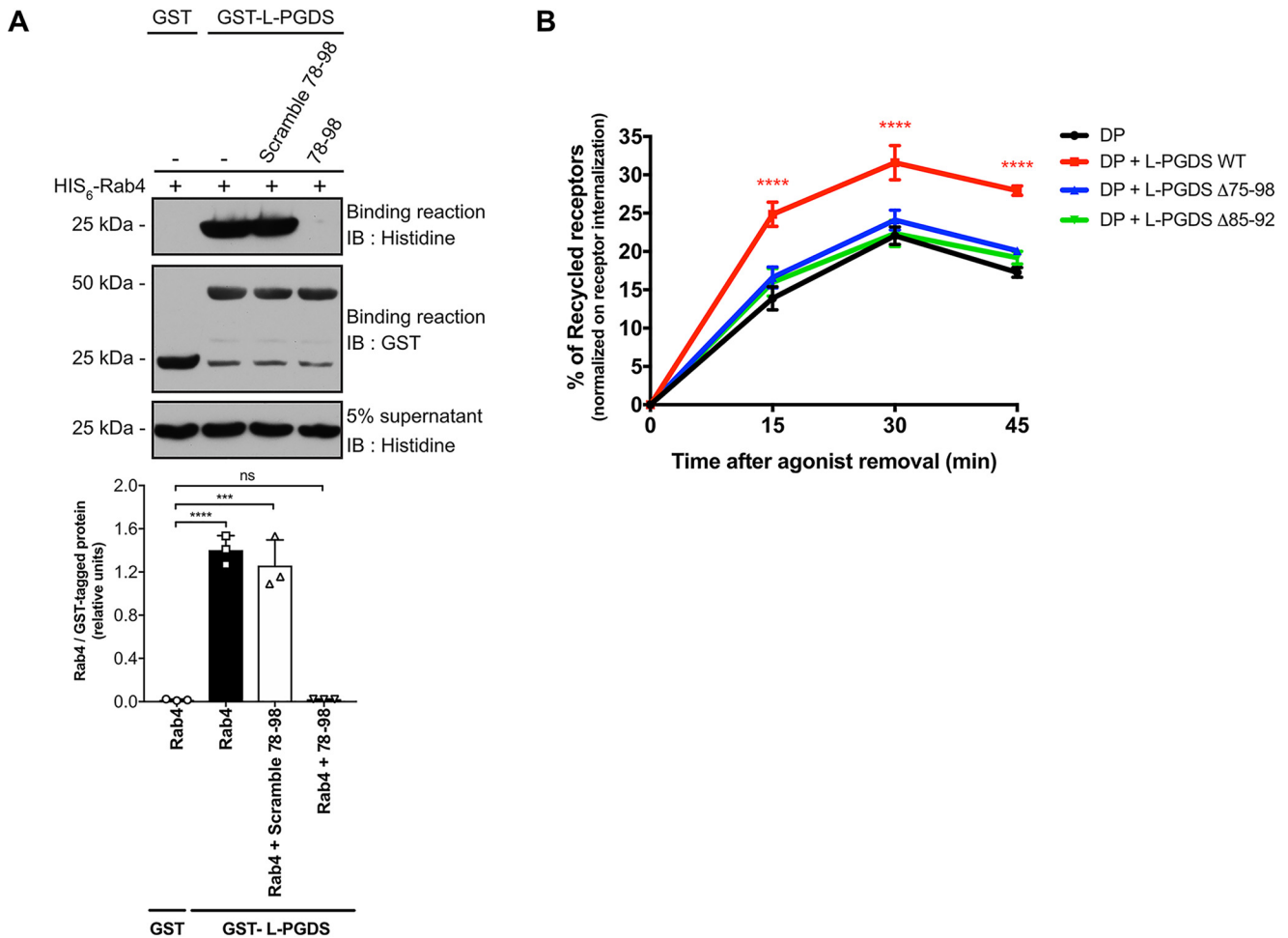
Figure 9. The interaction with Rab4 is necessary for L-PGDS to regulate DP1 recycling. *A*, peptides were incubated for 1 h with His$_6$-Rab4 prior to binding assays. Assays were carried out using purified GSH-Sepharose– bound GST-L-PGDS WT incubated with peptides and His$_6$-Rab4. The binding of Rab4 to L-PGDS was detected by immunoblotting using an anti-His antibody, and GST-L-PGDS was detected using an anti-GST antibody. The graph shows densitometry analyses performed on three different experiments. Rab4 pixels were normalized on L-PGDS pixels, and results are presented as -fold of these values (means ± S.D. (*error bars*)). ***, $p < 0.001$; ****, $p < 0.0001$; *ns*, not significant. *B*, HEK293 cells were co-transfected with pcDNA3-FLAG-DP1 and pcDNA3-L-PGDS, pcDNA3-L-PGDS Δ75–98, or pcDNA3-L-PGDS Δ85–92. Cells were treated with 1 μM PGD$_2$ for 30 min at 37 °C and then incubated in DMEM for the indicated time periods to prevent further internalization and to allow receptor recycling. Cell-surface expression of the receptor was detected by ELISA, and the percentage of receptor recycling was calculated. Results are means ± S.E. (*error bars*) of three separate experiments. ***, $p < 0.001$, ****, $p < 0.0001$.

the mechanism involved in the increased levels of activated Rab4 in the presence of L-PGDS.

Deletion mutagenesis studies led to the identification of two constructs (the L-PGDS Δ75–98 and Δ85–92 mutants) that could no longer bind Rab4. These L-PGDS mutants failed to regulate DP1 recycling, indicating that the L-PGDS–Rab4 interaction is required for this function. The L-PGDS–Rab4–binding domain was further confirmed by the ability of the L-PGDS 75–98 amino acid sequence fused to GST to interact with Rab4 and by the *in vitro* inhibition of the L-PGDS-Rab4 interaction by the L-PGDS 78–98 synthetic peptide.

We cannot state at the moment whether L-PGDS acts, for example, as a GEF, a holdase, or other conformational change–inducing binding partner on Rab4. L-PGDS does not display a Vps9 domain, a DENN domain, a multisubunit TRAPP complex, or a Sec2 domain that can be found in Rab GEFs (38, 51, 55, 56, 76, 82–84). Detection of GDP-GTP exchange or GTP-loading promotion by a protein is not necessarily indicative of a GEF protein *per se*. Indeed, as elegantly demonstrated by Gulbranson *et al.* (85), instead of functioning as a Rab GEF as pre-

viously postulated, RABIF/MSS4 is a holdase chaperone that is crucial for the expression of its cognate Rab GTPases. Solution NMR studies are under way in our laboratory to determine how L-PGDS binds to Rab4 and favors its activation.

In summary, we have discovered an original mechanism for the regulation of DP1 recycling by the synthase of its agonist, L-PGDS, which recruits Rab4 to the receptor and participates in the activation of the small GTPase.

Experimental procedures

Reagents

dase high-affinity antibody (3F10) was bought from Roche Applied Science. The monoclonal c-MYC antibody was from Biolegend. The anti-MYC-peroxidase high-affinity polyclonal antibody was from Abcam, whereas the anti-GST polyclonal antibody was from Bethyl Laboratories. The monoclonal anti-His was from Cell Signaling Technology. The polyclonal anti-HA, normal mouse, and rabbit IgG isotypic control antibodies, anti-GAPDH, anti-Rab4 (FL-213), and the protein G-agarose and A-agarose beads were purchased from Santa Cruz Biotechnology, Inc. The polyclonal and monoclonal anti-L-PGDS antibodies and PGD_2 were from Cayman Chemical Co. The Antarctic Phosphatase was from New England BioLabs, Inc. (M0289S). Alexa Fluor 633 goat anti-rabbit and ProLong® Gold antifade reagent were bought from Invitrogen.

Plasmid constructs

The cDNA fragment coding for human Rab4 was amplified by PCR from a human HeLa MATCH-MAKER cDNA library (Clontech) using the high-fidelity DNA polymerase (Phusion, New England Biolabs, Inc.) and the following primers: Rab4 forward (5′-GAG GAA TTC ATG TCC GAA ACC TAC GAT TTT TTG-3′) and Rab4 reverse (5′-GAG CTC GAG CTA ACA ACC ACA CTC CTG AGC-3′). The full-length fragment was digested with EcoRI and XhoI and ligated into pcDNA3-HA vector digested likewise. Site-directed mutagenesis was carried out by PCR. The Rab4S22N and Rab4Q67L mutants were prepared from the pcDNA3-HA-Rab4 construct by using these primers: Rab4S22N forward (5′-GGA AAT GCA GGA ACT GGC AAA AAT TGC TTA CTT CAT CAG-3′), Rab4S22N reverse (5′-CTG ATG AAC TAA GCA ATT TTT GCC AGT TCC TGC ATT TCC-3′), Rab4Q67L forward (5′-ACA GCA GGA CTA GAA CGA TTC AGG-3′), Rab4Q67L reverse (5′-CCT GAA TCG TTC TAG TCC TGC TGT-3′), and Rab4 forward and Rab4 reverse as mentioned previously. The fragments were ligated by the PCR extension method. The full-length mutant fragments were digested with EcoRI and XhoI and ligated into pcDNA3-HA digested with the same enzymes. The His_6-Rab4 construct was prepared from pcDNA3-HA-Rab4 by using the following primers: pRSETA Rab4 forward (5′-CTAG GGA TCC ATG TCC GAA ACC TAC GAT TTT TTG TTT AAG TTC-3′) and pRSETA Rab4 reverse (5′-CTAG GAA TTC CTA ACA ACC ACA CTC CTG AGC GTT CGG GGC CTG GGT GCG CCG CGG TGA CCT CAG-3′). The PCR fragment was digested with BamHI and EcoRI and inserted into pRSETA previously digested the same way. The GST-rabaptin construct was prepared by PCR from the human RABEP1 sequence-verified cDNA clone template purchased from GE Dharmacon (Clone ID: 6046320) with the use of the following primers: rabaptin forward (5′-CTAG GTC GAC ATG GCG CAG CCG GGC CCG GCT TCC CAG CCT-3′) and rabaptin reverse (5′-CTAG GTC GAC TCA TGT CTC AGG AAG CTG GTT AAT GTC TGT CAG TTT AGT ATC ATT CAG-3′). The PCR fragment was digested with SalI and inserted into pGEX-4T1 previously digested with SalI and treated with the Antarctic Phosphatase according to the manufacturer's instruction to prevent self-ligation of the vector. The pcDNA3-L-PGDS-HA, pcDNA3-L-PGDS-MYC, pGEX-4T1-L-PGDS, and pRSETA-LPGDS were produced as described previously (86). The

pcDNA3-FLAG-DP1 construct was generated as described earlier (53). The pcDNA3-L-PGDS-W43A/G47A-HA, pGEX4T1-DP1-CT, and pGEX-4T1-DP1-ICL1 were generated as described previously (61). The other ICLs of DP1 were subcloned as described previously (87).

Cell culture and transfections

HEK293 and HeLa cells were cultured in Dulbecco's modified Eagle's medium (DMEM) (Invitrogen) supplemented with 10% fetal bovine serum at 37 °C in a humidified atmosphere containing 5% CO_2. Transient transfection of HEK293 and HeLa cells grown to 50–70% confluence was performed using *Trans*IT®-LT1 reagent (Mirus) and Lipofectamine 2000 (Invitrogen), respectively, and according to the manufacturer's instructions. The total amount of DNA was kept constant by adding empty pcDNA3 vector per plate.

Immunoprecipitation

HEK293 cells were transiently transfected with the indicated constructs and were maintained as described above for 48 h. When stimulation was needed, cells were incubated in the presence of 1 μM PGD_2 for the desired times in serum-free DMEM containing 20 mM HEPES and 0.5% BSA before harvesting. The cells were then washed with ice-cold PBS and harvested in 400 μl of lysis buffer (150 mM NaCl, 50 mM Tris (pH 8.0), 0.5% deoxycholate, 0.1% SDS, 10 mM $Na_4P_2O_7$, 1% IGEPAL, and 5 mM EDTA or 1 mM $CaCl_2$, depending on the antibody used for the assay) supplemented with protease inhibitors (10 μM chymostatin, 10 μM leupeptin, 9 μM antipain, and 9 μM pepstatin) (Roche Applied Science). After a 1-h incubation at 4 °C, the lysates were centrifuged for 20 min at 13,500 × g at 4 °C. Proteins were immunoprecipitated using 1 μg of specific antibodies overnight. 40 μl of 50% protein G- or A-agarose beads were added to the lysates for 1 h the next morning. Samples were then centrifuged for 2 min in a microcentrifuge and washed three times with 1 ml of lysis buffer supplemented with protease inhibitors as mentioned above. 40 μl of SDS sample buffer was added to elute the immunoprecipitated proteins, followed by a 60-min incubation at room temperature. Initial lysates and immunoprecipitated proteins were analyzed by SDS-PAGE and immunoblotting. Endogenous immunoprecipitations were performed in HeLa cells. Cells were harvested and processed as described above, except proteins were immunoprecipitated using 5 μg of L-PGDS–specific or isotypic control IgG antibody, and 40 μl of 50% protein G-agarose beads overnight.

Recombinant protein production and pulldown analysis

All of the constructs in pGEX-4T1 vector (Amersham Biosciences) listed previously were used to produce GST-tagged fusion proteins in the Overexpress™ C41 (DE3) *Escherichia coli* strain (Avidis) as indicated by the manufacturer. Glutathione-Sepharose 4B (Amersham Biosciences) was used for protein purification, and the purified recombinant proteins were analyzed by SDS-PAGE followed by Coomassie Brilliant Blue R-250 staining. The pRSETA constructs were used to produce His-tagged fusion proteins using the Overexpress™ C41 system as mentioned above. The fusion proteins were purified using nickel-nitrilotriacetic acid-agarose resin (Qiagen) by fol-

lowing the manufacturer's instructions. 5 μg (0.5 μM final concentration) of glutathione-Sepharose–bound GST-tagged fusion proteins were incubated with 10 μg (1.5 μM final concentration) of the purified His-tagged proteins in binding buffer (10 mM Tris-HCl (pH 7.4), 150 mM NaCl, 10% glycerol, 0.5% IGEPAL, and 2 mM DTT) supplemented with protease inhibitors (10 μM chymostatin, 10 μM leupeptin, 9 μM antipain, and 9 μM pepstatin). The binding reactions were then washed three times with binding buffer. SDS sample buffer was added to each reaction before boiling the tubes for 5 min. All reactions were analyzed by Western blotting using specific antibodies as indicated. Where indicated, 5 μg of glutathione-Sepharose–bound GST-tagged fusion proteins were incubated with 300 μl of cell lysates. The cells were transfected with the indicated constructs, cultured, harvested, and lysed in the absence of EDTA as mentioned earlier, and the binding reactions were processed as mentioned above.

Immunofluorescence staining and confocal microscopy

For co-localization experiments, HeLa cells were plated directly onto coverslips previously coated with 0.1 mg/ml poly-L-lysine (Sigma-Aldrich) at a density of 7.5 $\times$ 10^4 cells/well in 6-well plates. The cells were then transiently transfected with the indicated constructs using Lipofectamine LTX (Thermo Fisher Scientific) according to the manufacturer's instructions. After 48 h, the cells were fixed with 4% paraformaldehyde in PBS, washed with PBS, permeabilized with 0.1% Triton X-100 in PBS, and blocked with 0.1% Triton X-100 in PBS containing 2% BSA. They were then incubated with primary antibodies diluted in blocking solution for 60 min, washed twice with 0.1% Triton X-100 in PBS, blocked with 0.1% Triton X-100 in PBS containing 2% BSA, and incubated with the appropriate secondary antibodies diluted in blocking solution for 60 min. The cells were then washed twice with 0.1% Triton X-100 in PBS followed by three washes with PBS. The coverslips were mounted using ProLong® Gold antifade reagent. Confocal microscopy was performed using a scanning confocal system (TCS SP8, Leica) coupled to an inverted microscope with a $\times$60 oil immersion objective (DMI8, Leica), and the images were processed using LAS X software (Leica).

Measurement of DP1 internalization and recycling

For quantification of receptor internalization, HEK293 cells were plated at 5 $\times$ 10^5 cells in 24-well plates pretreated with 0.1 mg/ml poly-L-lysine (Sigma). Cells were transfected the next day with the indicated constructs, and 48 h post-transfection, cells were stimulated with 1 μM PGD$_2$ or 10 μM isoproterenol for the desired times in serum-free DMEM containing 20 mM HEPES and 0.5% BSA, fixed in 3.7% formaldehyde/Tris-buffered saline (TBS) (20 mM Tris, pH 7.5, 150 mM NaCl, 1 mM CaCl$_2$) for 10 min, and then washed twice with TBS. Cells were blocked with TBS containing 1% BSA for 45 min to avoid nonspecific binding. A FLAG$_{M1}$-specific mAb was then added at a dilution of 1:2000 in 1% TBS-BSA for 60 min. Cells were then washed three times and blocked again with 1% TBS-BSA for 15 min. Cells were incubated with an alkaline phosphatase–conjugated goat anti-mouse antibody at a 1:10,000 dilution in 1% TBS-BSA for 60 min. The cells were then washed three

times before adding 250 μl of a colorimetric alkaline phosphatase substrate. The plates were incubated at 37 °C for 30 min, followed by the addition of 250 μl of 0.4 M NaOH to stop the reaction. 100 μl of the colorimetric reaction was collected, and the absorbance was measured at 405 nm using a spectrophotometer (Titertek Multiskan MCC/340, Labsystem). For quantification of receptor internalization using siRNAs, HEK293 cells or HeLa cells stably expressing the FLAG-DP1 receptor were plated at 5 $\times$ 10^5 and 3 $\times$ 10^5 cells, respectively, in 24-well plates and transfected the same day with the desired siRNAs. ELISAs were carried out as mentioned above 72 h post-transfection. For quantification of receptor recycling, cells were plated and transfected as described earlier and maintained for 48 h. Cells were then stimulated with 1 μM PGD$_2$ for 30 min at 37 °C to allow receptor internalization. Cells were washed once with PBS before adding DMEM containing 0.5% BSA and 20 mM HEPES to allow receptor recycling. Recycling was then stopped at the desired times, and cell-surface receptor expression was assessed as described above.

GTPγS-loading assays

Purified Rab4 protein concentration was estimated by comparing Coomassie staining with known BSA control concentrations on a 10% SDS-polyacrylamide gel. GTPγS loading was performed essentially as described by Jean *et al.* (88). Purified His$_6$-Rab4 (estimated 10 μM) was incubated in GTPase-loading buffer (40 μM GDP, 20 mM Tris-HCl, pH 7.4, 100 mM NaCl, 5 mM EDTA) at 30 °C for 10 min to allow loading of GDP. 10 mM MgCl$_2$ was then added to stabilize Rab4 GTPase in the GDP-loaded form. GTPγS exchange reactions were performed at room temperature by adding exchange buffer (0.5 mg/ml BSA, 5 μM GTPγS, 0.5 mM DTT, 5 mM MgCl$_2$, 100 mM NaCl, 20 mM Tris-HCl, pH 7.4, with or without 3 μM His$_6$-L-PGDS or L-PGDS peptides) to 3 μM Rab4-GDP in a total volume of 130 μl for the indicated time intervals. After the allotted GTPγS-loading time, 70 μl of ice-cold wash buffer (20 mM Tris-HCl, pH 7.4, 100 mM NaCl, 20 mM MgCl$_2$) was added to the mix. Pulldown assays using purified GST-rabaptin were carried out for 2 h as mentioned earlier. The binding reactions were then washed three times with ice-cold wash buffer and further processed as mentioned above.

Solid-phase peptide synthesis

Unless otherwise noted, all reactions were performed under nitrogen pressure. All solvents used were HPLC grade and were used without further purification. Water-sensitive reactions were performed in anhydrous solvents. TentaGel S RAM resin (0.22 mmol g^{-1}) was purchased from Rapp Polymere (Tübingen, Germany). All of the amino acid derivatives and coupling reagents were purchased from ChemImpex International (Wood Dale, IL). Piperidine and *N*-methylpyrrolidinone were obtained from A&C American Chemicals Ltd. (Saint-Laurent, Quebec, Canada). All other reagents were purchased from Sigma-Aldrich. The UPLC-MS analysis was performed on a Waters (Milford, MA) AQUITY H-Class separation module coupled with a Waters SQD2 mass spectrometer equipped with an analytical column BEH C18 (1.7 μm, 2.1 $\times$ 50 mm). Preparative HPLC was carried out using a Waters 2535 module with

an ACE C18 column (5 μm, 250 $\times$ 21.2 mm) (Canadian Life Science, Peterborough, Canada). The peptide syntheses were performed on an automated system using Tentagel S RAM resin. The resin was first loaded in reaction vessels on the Symphony-X peptide synthesizer (Gyros Protein Technologies, Tucson, AZ). The deprotection step was performed using 20% piperidine in *N,N*-dimethylformamide, and Fmoc amino acids were added in a 5-fold excess using HATU in the presence of DIPEA. Once all amino acids were coupled and the terminal Fmoc was removed, the peptides were cleaved from the polymer solid support using a mixture of TFA/H_2O/TIPS/EDT (92.5:2.5:2.5:2.5, v/v/v/v) with stirring for 3 h. The mixture was filtered and then precipitated in diethyl ether. The precipitated crude peptides were centrifuged, and the ether layer was removed by decantation. The crude peptides were dissolved in a mixture of water and acetonitrile, filtered, diluted with water, lyophilized, and then purified with a preparative HPLC. The fractions containing the pure peptide were pooled and lyophilized to yield the final peptides as white powders. The identity of the peptides was confirmed by MS.

siRNAs

The control nontargeting DsiRNA duplex (DS NC1) and the DsiRNA duplexes targeting the human Rab4 gene (HSC.RNAI.N004578.12.9 and 13.3), the negative control siRNA (Silencer Negative control 1, catalogue no. 4390843) and the siRNA targeting the human L-PGDS (PTGDS) gene (siRNA ID s11446 and CDS4/5) were purchased from IDT. HeLa cells stably expressing the FLAG-DP1 receptor were transfected with 200 nM oligonucleotide using the Lipofectamine 2000 transfection reagent (Invitrogen) according to the manufacturer's instructions. Cells were harvested as mentioned above, and protein expression was assessed by Western blotting 72 h post-transfection.

Transcreener GDP TR-FRET red assays

As indicated in the Transcreener GDP TR-FRET red assay's technical manual (BellBrook Labs LLC), the enzyme reactions were performed in a 10-μl volume containing purified His$_6$-Rab4 in the presence or absence of His$_6$-L-PGDS, both diluted in FRET assay buffer (25 mM Tris (pH 7.5), 2.5 mM MgCl$_2$, 0.5 mM EDTA, 0.5% DMSO, 0.01% SDS). The reactions were started by the addition of 10 μM GTP and carried out at room temperature for the indicated period of time. The reactions were then stopped by the addition of 10 μl of a 1$\times$ GDP detection mixture (8 nM GDP Antibody-Tb, 1$\times$ Stop and Detect Buffer C, 26.8 nM GDP HiLyte647 Tracer) according to the technical manual, bringing the final volume to 20 μl. The plate was rocked at room temperature for 90 min, and TR-FRET was measured. White 384-well microplates (AlphaPlate$^{\text{TM}}$-384 SW, PerkinElmer Life Sciences) were used, and FRET signals were recorded on an Infinite M1000 plate reader (TECAN). The terbium conjugate was excited at 320 nm, and emission was measured at 615 and 665 nm after a delay time of 150 μs and total integration time of 500 μs. All TR-FRET signals were expressed as TR-FRET ratios (665/615), and values in graphs are means of data of three separate experiments. The range of enzyme concentrations and time of assay were determined based on a previous publication from BellBrook Labs ([89]). Titration assays were done in 2-fold serial dilutions starting at a 10 μM enzyme concentration. Reactions were started as described above and mixed at room temperature for 60 min before adding the GDP detection mixture. IC$_{50}$ values calculated following titrations (Rab4, 80 nM; L-PGDS, 320 nM) were used as optimized enzyme concentrations in the time-course TR-FRET assays. All data were analyzed using GraphPad Prism using a four-parameter nonlinear regression curve fitting.

Statistical analysis

Statistical analysis was performed using Prism version 5.0 (GraphPad Software) using a two-tailed Student's t test or two-way analysis of variance with multiple comparisons. Data were considered significant when p values were <0.05 (*), <0.01 (**), <0.001 (***), or <0.0001 (****).

References

1. Hardy, C. C., Robinson, C., Tattersfield, A. E., and Holgate, S. T. (1984) The bronchoconstrictor effect of inhaled prostaglandin D$_2$ in normal and asthmatic men. *N. Engl. J. Med.* **311,** 209–213 CrossRef Medline
2. Ueno, R., Honda, K., Inoué, S., and Hayaishi, O. (1983) Prostaglandin D$_2$, a cerebral sleep-inducing substance in rats. *Proc. Natl. Acad. Sci. U.S.A.* **80,** 1735–1737 CrossRef Medline
3. Eguchi, N., Minami, T., Shirafuji, N., Kanaoka, Y., Tanaka, T., Nagata, A., Yoshida, N., Urade, Y., Ito, S., and Hayaishi, O. (1999) Lack of tactile pain (allodynia) in lipocalin-type prostaglandin D synthase-deficient mice. *Proc. Natl. Acad. Sci. U.S.A.* **96,** 726–730 CrossRef Medline
4. Matsuoka, T., Hirata, M., Tanaka, H., Takahashi, Y., Murata, T., Kabashima, K., Sugimoto, Y., Kobayashi, T., Ushikubi, F., Aze, Y., Eguchi, N., Urade, Y., Yoshida, N., Kimura, K., Mizoguchi, A., *et al.* (2000) Prostaglandin D$_2$ as a mediator of allergic asthma. *Science* **287,** 2013–2017 CrossRef Medline
5. Ishizuka, T., Matsui, T., Okamoto, Y., Ohta, A., and Shichijo, M. (2004) Ramatroban (BAY u 3405): a novel dual antagonist of TXA2 receptor and CRTh2, a newly identified prostaglandin D2 receptor. *Cardiovasc. Drug Rev.* **22,** 71–90 Medline
6. Gilroy, D. W., Colville-Nash, P. R., Willis, D., Chivers, J., Paul-Clark, M. J., and Willoughby, D. A. (1999) Inducible cyclooxygenase may have anti-inflammatory properties. *Nat. Med.* **5,** 698–701 CrossRef Medline
7. Ianaro, A., Ialenti, A., Maffia, P., Pisano, B., and Di Rosa, M. (2001) Role of cyclopentenone prostaglandins in rat carrageenin pleurisy. *FEBS Lett.* **508,** 61–66 CrossRef Medline
8. Vong, L., Ferraz, J. G. P., Panaccione, R., Beck, P. L., and Wallace, J. L. (2010) A pro-resolution mediator, prostaglandin D$_2$, is specifically up-regulated in individuals in long-term remission from ulcerative colitis. *Proc. Natl. Acad. Sci. U.S.A.* **107,** 12023–12027 CrossRef Medline
9. Gallant, M. A., Chamoux, E., Bisson, M., Wolsen, C., Parent, J.-L., Roux, S., and de Brum-Fernandes, A. J. (2010) Increased concentrations of prosta-

glandin D$_2$ during post-fracture bone remodeling. *J. Rheumatol.* **37,** 644–649 CrossRef Medline

10. Gallant, M. A., Samadfam, R., Hackett, J. A., Antoniou, J., Parent, J.-L., and de Brum-Fernandes, A. J. (2005) Production of prostaglandin D$_2$ by human osteoblasts and modulation of osteoprotegerin, RANKL, and cellular migration by DP and CRTH2 receptors. *J. Bone Miner. Res.* **20,** 672–681 Medline

11. Urade, Y., and Eguchi, N. (2002) Lipocalin-type and hematopoietic prostaglandin D synthases as a novel example of functional convergence. *Prostaglandins Other Lipid Mediat.* **68,** 375–382 Medline

12. Urade, Y., Ujihara, M., Horiguchi, Y., Igarashi, M., Nagata, A., Ikai, K., and Hayaishi, O. (1990) Mast cells contain spleen-type prostaglandin D synthetase. *J. Biol. Chem.* **265,** 371–375 Medline

13. Fujimori, K., Kanaoka, Y., Sakaguchi, Y., and Urade, Y. (2000) Transcriptional activation of the human hematopoietic prostaglandin D synthase gene in megakaryoblastic cells: roles of the oct-1 element in the 5′-flanking region and the AP-2 element in the untranslated exon 1. *J. Biol. Chem.* **275,** 40511–40516 CrossRef Medline

14. Tanaka, K., Ogawa, K., Sugamura, K., Nakamura, M., Takano, S., and Nagata, K. (2000) Cutting edge: differential production of prostaglandin D2 by human helper T cell subsets. *J. Immunol.* **164,** 2277–2280 CrossRef Medline

15. Urade, Y., Fujimoto, N., and Hayaishi, O. (1985) Purification and characterization of rat brain prostaglandin D synthetase. *J. Biol. Chem.* **260,** 12410–12415 Medline

16. Blödorn, B., Mäder, M., Urade, Y., Hayaishi, O., Felgenhauer, K., and Brück, W. (1996) Choroid plexus: the major site of mRNA expression for the β-trace protein (prostaglandin D synthase) in human brain. *Neurosci. Lett.* **209,** 117–120 CrossRef Medline

17. Eguchi, Y., Eguchi, N., Oda, H., Seiki, K., Kijima, Y., Matsu-ura, Y., Urade, Y., and Hayaishi, O. (1997) Expression of lipocalin-type prostaglandin D synthase (β-trace) in human heart and its accumulation in the coronary circulation of angina patients. *Proc. Natl. Acad. Sci. U.S.A.* **94,** 14689–14694 CrossRef Medline

18. Beuckmann, C. T., Gordon, W. C., Kanaoka, Y., Eguchi, N., Marcheselli, V. L., Gerashchenko, D. Y., Urade, Y., Hayaishi, O., and Bazan, N. G. (1996) Lipocalin-type prostaglandin D synthase (β-trace) is located in pigment epithelial cells of rat retina and accumulates within interphotoreceptor matrix. *J. Neurosci.* **16,** 6119–6124 CrossRef Medline

19. Gerena, R. L., Eguchi, N., Urade, Y., and Killian, G. J. (2000) Stage and region-specific localization of lipocalin-type prostaglandin D synthase in the adult murine testis and epididymis. *J. Androl.* **21,** 848–854 Medline

20. Tanaka, T., Urade, Y., Kimura, H., Eguchi, N., Nishikawa, A., and Hayaishi, O. (1997) Lipocalin-type prostaglandin D synthase (β-trace) is a newly recognized type of retinoid transporter. *J. Biol. Chem.* **272,** 15789–15795 CrossRef Medline

21. Beuckmann, C. T., Aoyagi, M., Okazaki, I., Hiroike, T., Toh, H., Hayaishi, O., and Urade, Y. (1999) Binding of biliverdin, bilirubin, and thyroid hormones to lipocalin-type prostaglandin D synthase. *Biochemistry* **38,** 8006–8013 CrossRef Medline

22. Mohri, I., Taniike, M., Okazaki, I., Kagitani-Shimono, K., Aritake, K., Kanekiyo, T., Yagi, T., Takikita, S., Kim, H.-S., Urade, Y., and Suzuki, K. (2006) Lipocalin-type prostaglandin D synthase is up-regulated in oligodendrocytes in lysosomal storage diseases and binds gangliosides. *J. Neurochem.* **97,** 641–651 CrossRef Medline

23. Boie, Y., Sawyer, N., Slipetz, D. M., Metters, K. M., and Abramovitz, M. (1995) Molecular cloning and characterization of the human prostanoid DP receptor. *J. Biol. Chem.* **270,** 18910–18916 CrossRef Medline

24. Hirai, H., Tanaka, K., Yoshie, O., Ogawa, K., Kenmotsu, K., Takamori, Y., Ichimasa, M., Sugamura, K., Nakamura, M., Takano, S., and Nagata, K. (2001) Prostaglandin D$_2$ selectively induces chemotaxis in T helper type 2 cells, eosinophils, and basophils via seven-transmembrane receptor CRTH2. *J. Exp. Med.* **193,** 255–261 CrossRef Medline

25. Lebon, G., and Tate, C. G. (2012) [G protein-coupled receptors in the spotlight]. *Med. Sci.* (*Paris*) **28,** 876–882 CrossRef Medline

26. Lachance, V., Degrandmaison, J., Marois, S., Robitaille, M., Génier, S., Nadeau, S., Angers, S., and Parent, J.-L. (2014) Ubiquitylation and activa-

tion of a Rab GTPase is promoted by a β$_2$AR-HACE1 complex. *J. Cell Sci.* **127,** 111–123 CrossRef Medline

27. Costanzi, S., Tikhonova, I. G., Harden, T. K., and Jacobson, K. A. (2009) Ligand and structure-based methodologies for the prediction of the activity of G protein-coupled receptor ligands. *J. Comput. Aided Mol. Des.* **23,** 747–754 CrossRef Medline

28. Pierce, K. L., Premont, R. T., and Lefkowitz, R. J. (2002) Seven-transmembrane receptors. *Nat. Rev. Mol. Cell Biol.* **3,** 639–650 CrossRef Medline

29. Ritter, S. L., and Hall, R. A. (2009) Fine-tuning of GPCR activity by receptor-interacting proteins. *Nat. Rev. Mol. Cell Biol.* **10,** 819–830 CrossRef Medline

30. Magalhaes, A. C., Dunn, H., and Ferguson, S. S. (2012) Regulation of GPCR activity, trafficking and localization by GPCR-interacting proteins. *Br. J. Pharmacol.* **165,** 1717–1736 CrossRef Medline

31. Esseltine, J. L., Dale, L. B., and Ferguson, S. S. G. (2011) Rab GTPases bind at a common site within the angiotensin II type I receptor carboxyl-terminal tail: evidence that Rab4 regulates receptor phosphorylation, desensitization, and resensitization. *Mol. Pharmacol.* **79,** 175–184 CrossRef Medline

32. Hamelin, E., Thériault, C., Laroche, G., and Parent, J.-L. (2005) The intracellular trafficking of the G protein-coupled receptor TPβ depends on a direct interaction with Rab11. *J. Biol. Chem.* **280,** 36195–36205 CrossRef Medline

33. Parent, A., Hamelin, E., Germain, P., and Parent, J.-L. (2009) Rab11 regulates the recycling of the β2-adrenergic receptor through a direct interaction. *Biochem. J.* **418,** 163–172 CrossRef Medline

34. Dateyama, I., Sugihara, Y., Chiba, S., Ota, R., Nakagawa, R., Kobayashi, T., and Itoh, H. (2018) RABL2 positively controls localization of GPCRs in mammalian primary cilia. *J Cell Sci.* **132,** jcs224428 CrossRef Medline

35. Seachrist, J. L., and Ferguson, S. S. G. (2003) Regulation of G protein-coupled receptor endocytosis and trafficking by Rab GTPases. *Life Sci.* **74,** 225–235 CrossRef Medline

36. Dong, C., Yang, L., Zhang, X., Gu, H., Lam, M. L., Claycomb, W. C., Xia, H., and Wu, G. (2010) Rab8 interacts with distinct motifs in α$_{2B}$- and β$_2$-adrenergic receptors and differentially modulates their transport. *J. Biol. Chem.* **285,** 20369–20380 CrossRef Medline

37. Li, C., Wei, Z., Fan, Y., Huang, W., Su, Y., Li, H., Dong, Z., Fukuda, M., Khater, M., and Wu, G. (2017) The GTPase Rab43 controls the anterograde ER-Golgi trafficking and sorting of GPCRs. *Cell Rep.* **21,** 1089–1101 CrossRef Medline

38. Cherfils, J., and Zeghouf, M. (2013) Regulation of small GTPases by GEFs, GAPs, and GDIs. *Physiol. Rev.* **93,** 269–309 CrossRef Medline

39. Hutagalung, A. H., and Novick, P. J. (2011) Role of Rab GTPases in membrane traffic and cell physiology. *Physiol. Rev.* **91,** 119–149 CrossRef Medline

40. Stenmark, H. (2009) Rab GTPases as coordinators of vesicle traffic. *Nat. Rev. Mol. Cell Biol.* **10,** 513–525 CrossRef Medline

41. Wandinger-Ness, A., and Zerial, M. (2014) Rab proteins and the compartmentalization of the endosomal system. *Cold Spring Harb. Perspect. Biol.* **6,** a022616 CrossRef Medline

42. Bhuin, T., and Roy, J. K. (2014) Rab proteins: the key regulators of intracellular vesicle transport. *Exp. Cell Res.* **328,** 1–19 CrossRef Medline

43. Wang, G., and Wu, G. (2012) Small GTPase regulation of GPCR anterograde trafficking. *Trends Pharmacol. Sci.* **33,** 28–34 CrossRef Medline

44. Pfeffer, S. R. (2001) Rab GTPases: specifying and deciphering organelle identity and function. *Trends Cell Biol.* **11,** 487–491 CrossRef Medline

45. Christoforidis, S., and Zerial, M. (2000) Purification and identification of novel Rab effectors using affinity chromatography. *Methods* **20,** 403–410 CrossRef Medline

46. Zhen, Y., and Stenmark, H. (2015) Cellular functions of Rab GTPases at a glance. *J. Cell Sci.* **128,** 3171–3176 CrossRef Medline

47. Blümer, J., Rey, J., Dehmelt, L., Mazel, T., Wu, Y.-W., Bastiaens, P., Goody, R. S., and Itzen, A. (2013) RabGEFs are a major determinant for specific Rab membrane targeting. *J. Cell Biol.* **200,** 287–300 CrossRef Medline

48. Pfeffer, S. R. (2013) Rab GTPase regulation of membrane identity. *Curr. Opin. Cell Biol.* **25,** 414–419 CrossRef Medline

49. Segev, N. (2001) Ypt/rab gtpases: regulators of protein trafficking. *Sci. STKE* **2001,** re11 CrossRef Medline

ASBMB

J. Biol. Chem. (2019) 294(45) 16865–16883 **16881**

50. Bos, J. L., Rehmann, H., and Wittinghofer, A. (2007) GEFs and GAPs: critical elements in the control of small G proteins. *Cell* **129,** 865–877 CrossRef Medline

51. Ishida, M., Oguchi, M. E., and Fukuda, M. (2016) Multiple types of guanine nucleotide exchange factors (GEFs) for Rab small GTPases. *Cell Struct. Funct.* **41,** 61–79 CrossRef Medline

52. Yudowski, G. A., Puthenveedu, M. A., Henry, A. G., and von Zastrow, M. (2009) Cargo-mediated regulation of a rapid Rab4-dependent recycling pathway. *Mol. Biol. Cell* **20,** 2774–2784 CrossRef Medline

53. Gallant, M. A., Slipetz, D., Hamelin, E., Rochdi, M. D., Talbot, S., de Brum-Fernandes, A. J., and Parent, J.-L. (2007) Differential regulation of the signaling and trafficking of the two prostaglandin D2 receptors, prostanoid DP receptor and CRTH2. *Eur. J. Pharmacol.* **557,** 115–123 CrossRef Medline

54. Koch, D., Rai, A., Ali, I., Bleimling, N., Friese, T., Brockmeyer, A., Janning, P., Goud, B., Itzen, A., Müller, M. P., and Goody, R. S. (2016) A pull-down procedure for the identification of unknown GEFs for small GTPases. *Small GTPases* **7,** 93–106 CrossRef Medline

55. Müller, M. P., and Goody, R. S. (2018) Molecular control of Rab activity by GEFs, GAPs and GDI. *Small GTPases* **9,** 5–21 CrossRef Medline

56. Yoshimura, S., Gerondopoulos, A., Linford, A., Rigden, D. J., and Barr, F. A. (2010) Family-wide characterization of the DENN domain Rab GDP-GTP exchange factors. *J. Cell Biol.* **191,** 367–381 CrossRef Medline

57. Do, M. T., Chai, T. F., Casey, P. J., and Wang, M. (2017) Isoprenylcysteine carboxylmethyltransferase function is essential for RAB4A-mediated integrin β3 recycling, cell migration and cancer metastasis. *Oncogene* **36,** 5757–5767 CrossRef Medline

58. Barbarin, A., and Frade, R. (2011) Procathepsin L secretion, which triggers tumour progression, is regulated by Rab4a in human melanoma cells. *Biochem. J.* **437,** 97–107 CrossRef Medline

59. Arsenault, D., Lucien, F., and Dubois, C. M. (2012) Hypoxia enhances cancer cell invasion through relocalization of the proprotein convertase furin from the *trans*-Golgi network to the cell surface. *J. Cell Physiol.* **227,** 789–800 CrossRef Medline

60. Frittoli, E., Palamidessi, A., Marighetti, P., Confalonieri, S., Bianchi, F., Malinverno, C., Mazzarol, G., Viale, G., Martin-Padura, I., Garré, M., Parazzoli, D., Mattei, V., Cortellino, S., Bertalot, G., Di Fiore, P. P., and Scita, G. (2014) A RAB5/RAB4 recycling circuitry induces a proteolytic invasive program and promotes tumor dissemination. *J. Cell Biol.* **206,** 307–328 CrossRef Medline

61. Binda, C., Génier, S., Cartier, A., Larrivée, J.-F., Stankova, J., Young, J. C., and Parent, J.-L. (2014) A G protein-coupled receptor and the intracellular synthase of its agonist functionally cooperate. *J. Cell Biol.* **204,** 377–393 CrossRef Medline

62. Génier, S., Degrandmaison, J., Moreau, P., Labrecque, P., Hébert, T. E., and Parent, J.-L. (2016) Regulation of GPCR expression through an interaction with CCT7, a subunit of the CCT/TRiC complex. *Mol. Biol. Cell* **27,** 3800–3812 CrossRef Medline

63. Roy, S. J., Glazkova, I., Fréchette, L., Iorio-Morin, C., Binda, C., Pétrin, D., Trieu, P., Robitaille, M., Angers, S., Hébert, T. E., and Parent, J.-L. (2013) Novel, gel-free proteomics approach identifies RNF5 and JAMP as modulators of GPCR stability. *Mol. Endocrinol.* **27,** 1245–1266 CrossRef Medline

64. Lachance, V., Cartier, A., Génier, S., Munger, S., Germain, P., Labrecque, P., and Parent, J.-L. (2011) Regulation of β2-adrenergic receptor maturation and anterograde trafficking by an interaction with Rab geranylgeranyltransferase: modulation of Rab geranylgeranylation by the receptor. *J. Biol. Chem.* **286,** 40802–40813 CrossRef Medline

65. Dale, L. B., Seachrist, J. L., Babwah, A. V., and Ferguson, S. S. G. (2004) Regulation of angiotensin II type 1A receptor intracellular retention, degradation, and recycling by Rab5, Rab7, and Rab11 GTPases. *J. Biol. Chem.* **279,** 13110–13118 CrossRef Medline

66. Hammad, M. M., Kuang, Y.-Q., Morse, A., and Dupré, D. J. (2012) Rab1 interacts directly with the β2-adrenergic receptor to regulate receptor anterograde trafficking. *Biol. Chem.* **393,** 541–546 CrossRef Medline

67. Mulvaney, E. P., O'Meara, F., Khan, A. R., O'Connell, D. J., and Kinsella, B. T. (2017) Identification of α-helix 4 (α4) of Rab11a as a novel Rab11-binding domain (RBD): interaction of Rab11a with the prostacyclin recep-

tor. *Biochim. Biophys. Acta Mol. Cell Res.* **1864,** 1819–1832 CrossRef Medline

68. Langemeyer, L., Nunes Bastos, R., Cai, Y., Itzen, A., Reinisch, K. M., and Barr, F. A. (2014) Diversity and plasticity in Rab GTPase nucleotide release mechanism has consequences for Rab activation and inactivation. *Elife* **3,** e01623 Medline

69. Kanie, T., and Jackson, P. K. (2018) Guanine nucleotide exchange assay using fluorescent MANT-GDP. *Bio Protoc.* **8,** e2795 CrossRef Medline

70. Esseltine, J. L., Ribeiro, F. M., and Ferguson, S. S. G. (2012) Rab8 modulates metabotropic glutamate receptor subtype 1 intracellular trafficking and signaling in a protein kinase C-dependent manner. *J. Neurosci.* **32,** 16933–16942a CrossRef Medline

71. O'Keeffe, M. B., Reid, H. M., and Kinsella, B. T. (2008) Agonist-dependent internalization and trafficking of the human prostacyclin receptor: a direct role for Rab5a GTPase. *Biochim. Biophys. Acta* **1783,** 1914–1928 CrossRef Medline

72. Seachrist, J. L., Anborgh, P. H., and Ferguson, S. S. (2000) β2-Adrenergic receptor internalization, endosomal sorting, and plasma membrane recycling are regulated by Rab GTPases. *J. Biol. Chem.* **275,** 27221–27228 CrossRef Medline

73. Smythe, E. (2002) Direct interactions between rab GTPases and cargo. *Mol. Cell* **9,** 205–206 CrossRef Medline

74. Wikström, K., Reid, H. M., Hill, M., English, K. A., O'Keeffe, M. B., Kimbembe, C. C., and Kinsella, B. T. (2008) Recycling of the human prostacyclin receptor is regulated through a direct interaction with Rab11a GTPase. *Cell. Signal.* **20,** 2332–2346 CrossRef Medline

75. Seabra, M. C., and Wasmeier, C. (2004) Controlling the location and activation of Rab GTPases. *Curr. Opin. Cell Biol.* **16,** 451–457 CrossRef Medline

76. Barr, F., and Lambright, D. G. (2010) Rab GEFs and GAPs. *Curr. Opin. Cell Biol.* **22,** 461–470 CrossRef Medline

77. Ginsberg, S. D., Mufson, E. J., Alldred, M. J., Counts, S. E., Wuu, J., Nixon, R. A., and Che, S. (2011) Upregulation of select rab GTPases in cholinergic basal forebrain neurons in mild cognitive impairment and Alzheimer's disease. *J. Chem. Neuroanat.* **42,** 102–110 CrossRef Medline

78. Soejima, N., Ohyagi, Y., Nakamura, N., Himeno, E., Iinuma, K. M., Sakae, N., Yamasaki, R., Tabira, T., Murakami, K., Irie, K., Kinoshita, N., LaFerla, F. M., Kiyohara, Y., Iwaki, T., and Kira, J. (2013) Intracellular accumulation of toxic turn amyloid-β is associated with endoplasmic reticulum stress in Alzheimer's disease. *Curr. Alzheimer. Res.* **10,** 11–20 CrossRef Medline

79. Caza, T. N., Fernandez, D. R., Talaber, G., Oaks, Z., Haas, M., Madaio, M. P., Lai, Z.-W., Miklossy, G., Singh, R. R., Chudakov, D. M., Malorni, W., Middleton, F., Banki, K., and Perl, A. (2014) HRES-1/Rab4-mediated depletion of Drp1 impairs mitochondrial homeostasis and represents a target for treatment in SLE. *Ann. Rheum. Dis.* **73,** 1888–1897 CrossRef Medline

80. Hu, C.-T., Wu, J.-R., and Wu, W.-S. (2013) The role of endosomal signaling triggered by metastatic growth factors in tumor progression. *Cell. Signal.* **25,** 1539–1545 CrossRef Medline

81. Ferrándiz-Huertas, C., Fernández-Carvajal, A., and Ferrer-Montiel, A. (2011) Rab4 interacts with the human P-glycoprotein and modulates its surface expression in multidrug resistant K562 cells. *Int. J. Cancer* **128,** 192–205 CrossRef Medline

82. Delprato, A., and Lambright, D. G. (2007) Structural basis for Rab GTPase activation by VPS9 domain exchange factors. *Nat. Struct. Mol. Biol.* **14,** 406–412 CrossRef Medline

83. Marat, A. L., Dokainish, H., and McPherson, P. S. (2011) DENN domain proteins: regulators of Rab GTPases. *J. Biol. Chem.* **286,** 13791–13800 CrossRef Medline

84. Zhang, X., He, X., Fu, X.-Y., and Chang, Z. (2006) Varp is a Rab21 guanine nucleotide exchange factor and regulates endosome dynamics. *J. Cell Sci.* **119,** 1053–1062 CrossRef Medline

85. Gulbranson, D. R., Davis, E. M., Demmitt, B. A., Ouyang, Y., Ye, Y., Yu, H., and Shen, J. (2017) RABIF/MSS4 is a Rab-stabilizing holdase chaperone required for GLUT4 exocytosis. *Proc. Natl. Acad. Sci. U.S.A.* **114,** E8224–E8233 CrossRef Medline

86. Mathurin, K., Gallant, M. A., Germain, P., Allard-Chamard, H., Brisson, J., Iorio-Morin, C., de Brum Fernandes, A., Caron, M. G., Laporte, S. A., and

Parent, J.-L. (2011) An interaction between L-prostaglandin D synthase and arrestin increases PGD2 production. *J. Biol. Chem.* **286,** 2696–2706 CrossRef Medline

87. Parent, A., Roy, S. J., Iorio-Morin, C., Lépine, M.-C., Labrecque, P., Gallant, M. A., Slipetz, D., and Parent, J.-L. (2010) ANKRD13C acts as a molecular chaperone for G protein-coupled receptors. *J. Biol. Chem.* **285,** 40838–40851 CrossRef Medline

88. Jean, S., Cox, S., Schmidt, E. J., Robinson, F. L., and Kiger, A. (2012) Sbf/MTMR13 coordinates PI(3)P and Rab21 regulation in endocytic control of cellular remodeling. *Mol. Biol. Cell* **23,** 2723–2740 CrossRef Medline

89. Reichman, M., Schabdach, A., Kumar, M., Zielinski, T., Donover, P. S., Laury-Kleintop, L. D., and Lowery, R. G. (2015) A high-throughput assay for Rho guanine nucleotide exchange factors based on the transcreener GDP assay. *J. Biomol. Screen.* **20,** 1294–1299 CrossRef Medline

ASBMB

J. Biol. Chem. (2019) 294(45) 16865–16883 **16883**